MICROWAVE LANDING SYSTEM (MLS)
MICROSTRIP ANTENNA STUDY
TP5438E

Prepared for:
Transportation Development Centre
April, 1984

By: Stuart G. Bailey
Canadian Astronautics Limited

The contents of this report reflect the views of the contractor and not necessarily the official views or policies of the Transportation Development Centre.

REPORT DOCUMENTATION FORM

1. Transport Canada Report No.	2. TDC Project No.	3. Recipient's Catalogue No.
TP5438E	6014	

4. Title and Subtitle	5. Report Date
MICROWAVE LANDING SYSTEM (MLS) MICROSTRIP ANTENNA STUDY	April, 1984
	6. Performing Organization Report No.

7. Author(s)	8. Transport Canada File No.
Stuart G. Bailey	D1455-153-4

9. Performing Organization Name and Address	10. DSS File No.
Canadian Astronautics Ltd. 1050 Morrison Dr. Ottawa, Ont. K2H 8K7	12SD.58200-3-3504
	11. DSS or Transport Canada Contract No.
	OSD83-00041

12. Sponsoring Agency Name and Address	13. Type of Report and Period Covered
Transportation Development Centre (TDC) 1000 Sherbrooke St. West Suite 2421 Montreal, P.Q. H3A 2R3	Final, July 1983-April 1984
	14. Sponsoring Agency Code

15. Supplementary Notes	16. TDC Project Officer
	Micha Avni

17. Abstract

The Microwave Landing System (MLS) defined by the International Civil Aviation Organization is to be the standard instrument for landing aircraft in reduced visibility. At present, the slotted waveguide type antenna has been used to provide the azimuth coverage of the MLS system. However, a microstrip antenna could provide a more cost-effective solution to the problem.

A study of the possibilities of using a microstrip antenna is reported. Various microstrip antenna designs were analyzed and a suitable design was chosen. This design consisted of a linear array of rectangular patch radiators. The rectangular microstrip patch radiator was analyzed theoretically and experimentally and some design equations were given. The correlation between theory and experiment was good in most case and Lewin's theory on mutual coupling corresponded well with the experimental measurements made. Finally, a basic design concept was outlined and some typical performance parameters were given.

The patch array antenna proved easy to design and manufacture, providing the correct polarization, gain and VSWR.

This study concludes that a microstrip antenna can be produced to meet the requirements of an MLS azimuth subsystem antenna and that it can be a cheaper alternative to a slotted waveguide antenna. Also, it will be easier to manufacture, be repeatable, and contribute to a more frangible system.

18. Key Words	19. Distribution Statement
MICROWAVE LANDING SYSTEM, MLS MICROSTRIP ANTENNA	Limited number of copies available from Transportation Development Centre

20. Security Classification (of this report)	21. Security Classification (of this page)	22. No. of Pages	23. Price
UNCLASSIFIED	UNCLASSIFIED	80	NIL

TDC/CDT 79-005

FORMULE DE DOCUMENTATION POUR RAPPORT

1 N° du rapport Transports Canada	2 N° de l'étude — CDT	3 N° de catalogue du destinataire
TP5438E	6014	

4 Titre et sous-titre	5 Date du rapport
MICROWAVE LANDING SYSTEM (MLS) MICROSTRIP ANTENNA STUDY	Avril 1984
	6 N° du rapport de l'organisme exécutant

7 Auteur(s)	8 N° de dossier Transports Canada
Stuart G. Bailey	D1455-153-4

9 Nom et adresse de l'organisme exécutant	10 N° de dossier — ASC
Canadian Astronautics Ltd. 1050 Morrison Drive Ottawa, Ontario K2H 8K7	12SD.T8200-3-3504
	11 N° de contrat — ASC ou Transports Canada
	OSD83-00041

12 Nom et adresse de l'organisme parrain	13 Genre de rapport et période visée
Centre de développement des transports (CDT) 1000 ouest, rue Sherbrooke Suite 2421 Montréal, Québec H3A 2R3	Final Juillet 1983 - avril 1984
	14 Code de l'organisme parrain
	6014
15 Remarques additionnelles	16 Agent de projet — CDT
	Micha Avni

17 Résumé

Le système d'atterrissage hyperfréquence est le système standard adopté par l'Organisation de l'aviation civile internationale pour l'atterrissage des aéronefs dans des conditions de visibilité réduite. Actuellement, la couverture azimutale est obtenue à l'aide d'une antenne du type guide d'ondes à fentes. Toutefois, une antenne à microrubans serait moins coûteuse à utiliser.

Les résultats d'une étude sur la possibilité d'utiliser une antenne à microrubans sont rapportés ici. Divers types d'antennes à microrubans ont été examinés et un type approprié a été choisi. Celui-ci est constitué d'un alignement de radiateurs en plaquettes rectangulaires. La plaquette rectangulaire à microrubans a été étudiée théoriquement et expérimentalement et certaines équations de conception sont données. L'accord entre la théorie et l'expérience est bon dans la plupart des cas et la théorie de Lewin sur le couplage mutuel décrit bien les résultats expérimentaux. Enfin, un modèle d'antenne simple est décrit et certains paramètres de performance typiques sont donnés.

L'antenne à alignement de plaquettes s'est révélée facile à concevoir et à fabriquer et procure la polarisation, le gain et le ROS désirés.

La conclusion de cette étude est qu'on peut fabriquer une antenne à microrubans pouvant servir de sous-système d'antenne azimutale hyperfréquence et qu'elle est moins coûteuse qu'une antenne en guide d'ondes à fentes. De plus, de construction simple, elle peut être fabriquée à plusieurs exemplaires et elle est plus frangible.

18 Mots-clés	19 Diffusion
Système d'aterrissage hyperfréquence (MLS) Etude sur les antennes à microrubans.	Le CDT dispose d'un nombre limité de copies

20 Classification de sécurité (de ce rapport)	21 Classification de sécurité (de cette page)	22 Nombre de pages	23 Prix
non-classifié	non-classifiée	80	Nil

CDT/TDC 79-005

ACKNOWLEDGEMENT

The author would like to acknowledge the work of Vrage Minassian, formerly of Canadian Astronautics Ltd., who contributed greatly to this study.

TABLE OF CONTENTS

		Page
1.0	**INTRODUCTION**	1-1
	1.1 REQUIREMENTS	1-2
	1.2 OBJECTIVES OF THE STUDY	1-3
2.0	**ALTERNATIVE MICROSTRIP ARRAY ANTENNAE**	2-1
	2.1 RESONANT ELEMENT ARRAYS	2-1
	2.1.1 LINEAR ARRAY OF MICROSTRIP PATCHES	2-1
	2.1.2 SERIES FEEDING RESONANT ARRAY	2-5
	2.2 TRAVELLING WAVE ARRAYS	2-13
	2.2.1 RADIATION THROUGH SLOTS IN TRAVELLING WAVE ANTENNA	2-13
	2.2.2 FRANKLIN ANTENNA	2-20
	2.2.3 CHAIN ANTENNA	2-23
	2.3 CONCLUSIONS ON ALTERNATIVE MICROSTRIP ANTENNAE	2-25
3.0	**ANALYSIS OF A RECTANGULAR PATCH RADIATOR**	3-1
	3.1 APERTURE RADIATION FROM A SINGLE MICROSTRIP RECTANGULAR PATCH ELEMENT	3-1
	3.2 RADIATION CONDUCTANCE	3-5
	3.3 DIRECTIVITY	3-7
	3.4 SLOT CAPACITANCE	3-7
	3.5 EQUIVALENT NETWORK	3-8
4.0	**EXPERIMENTAL EVALUATION OF MICROSTRIP ANTENNA**	4-1
	4.1 MEASUREMENTS TO DETERMINE A SUITABLE COAXIAL TO MICROSTRIP TRANSITION	4-1
	4.2 INSERTION LOSS MEASUREMENTS	4-5
	4.3 MEASUREMENTS OF RETURN LOSS PARAMETER OF A SINGLE RECTANGULAR PATCH	4-7
	4.3.1 DIMENSIONS OF RECTANGULAR PATCH	4-9
	4.4 EXPERIMENTAL RESULTS OF RETURN LOSS $\lvert S_{11} \rvert^2$	4-10
	4.5 MEASUREMENT OF $\lvert S_{12} \rvert$ (COUPLING PARAMETER)	4-13
	4.6 CROSS POLARIZATION MEASUREMENTS	4-18

TABLE OF CONTENTS, continued

	Page
5.0 4 ELEMENT SYNTHSIS OF PATCH RADIATORS	5-1
5.1 DESIGN APPROACH	5-1
6.0 MLS MICROSTRIP ANTENNA - BASIC DESIGN CONCEPTS	6-1
6.1 PATTERN SYNTHESISARRAYS	6-1
6.2 PATCH ELEMENT CHARACTERISTICS	6-1
6.3 ANTENNA PERFORMANCERNATIVE MICROSTRIP ANTENNAE	6-5
7.0 CONCLUSIONS	7-1
8.0 REFERENCES	8-1

LIST OF FIGURES

		Page
2.1	Linear Array of Microstrip Elements	2-1
2.1.1-1a	H-Plane Radiation Pattern of Four-Element Microstrip Antenna	2-3
2.1.1-1b	E-Plane Radiation Pattern of Four-Element Microstrip Array	2-3
2.1.1-2	40 GHz Microstrip Array Antenna	2-4
2.1.1-3	E-Plane and H-Plane Patterns of a 4 x 4 Element Microstrip Array	2-6
2.1.2-1	Basis Series Fed Element	2-7
2.1.2-2	Linear Array of Series Fed Elements	2-7
2.1.2-3	Sketch of Microstrip Feder Showing the ith Stub and Associated Electrical Parameters	2-9
2.2.1-1	Electric Field of the Microstrip and Equivalent Magnetic Currents	2-14
2.2.1-2	Geometry for the Calculation of the Travelling Wave Antenna	2-15
2.2.1-3	Microstrip Antenna and its Near Field	2-17
2.2.1-4	Stubs Neutralizing the Fringe Capacitance	2-19
2.2.2-1	Franklin Antenna Configuration	2-21
2.2.2-2	Franklin-type Planar Array Antenna	2-22
2.2.3-1	Microstrip Chain Antenna	2-24
2.2.3-2	The Structure of a Printed Circuit Radio Link Antenna for 1.7...1.9 GHz	2-26
2.2.3-3	Calculated E-Plane Radiation Platterns of the Radio Link Antenna	2-26
3.1-1	Rectangular Microstrip Patch Antenna	3-2
3.1-2	Microstrip Antenna Represented as Two Radiating Slots with the Slot Geometry and Coordinate System	3-4
3.2-1	Strip Width versus Radiation Conductance	3-6
3.5-1	Equivalent Network of Microstrip Radiating Element	3-9

LIST OF FIGURES, continued

Figure No.		Page
4.1-1	Coaxial to Microstrip Transition via a Short Post	4-2
4.1-2	Horizontal Plane Coaxial to Microstrip Transition	4-3
4.1-3	Compling Detail of Horizontal Plane Transition	4-4
4.2-1	Experimental Setup for Measuring Insertion Loss	4-6
4.2-2	A Rectangular Patch Radiator with Feeder-lines (128Ω) and 50Ω Microstrip Transition Line	4-8
4.1-1	Return Loss versus Swept Frequency at 5 GHz	4-11
4.5-1	H-Plane Coupling of 2 Rectangular Patches	4-14
4.5-2	E-Plane Coupling of 2 Rectangular Patches	4-15
4.5-3	E-Plane Side Coupling of 2 Rectangular Patches	4-16
4.6-1	Cross Polarization of EΦ Component of Electric Field at Two Orthogonal Planes	4-19
6.0-1	MLS Azimuth Antenna	6-2
6.2-1	Equivalent Network of Linear Patch Array	6-3
6.3-1	Radiation Pattern for 32 Element Patch Array	6-6

1.0 INTRODUCTION

The Microwave Landing System defined by the International Civil Aviation Organization is to be the standard instrument for landing aircraft in reduced visibility. A significant level of effort has been expended by many countries in evaluating and developing these systems.

At the present time the antennae employed are of the slotted waveguide type. These provide a reliable, yet heavy and high cost solution to the problem. An alternative technique, as yet untried, is to use a microstrip antenna.

A further consideration is the frangibility of the antenna. The slotted waveguide antenna is a non-frangible system; however, the microstrip antenna will be a light, inexpensive alternative which would contribute greatly to a frangible system.

The microstrip antenna is formed from a TEM line transmission medium, usually a dielectric sheet with a ground plane on one side and a distribution circuit on the other side. Because of the dielectric the electromagnetic fields are largely contained between the two conductors. Such a system lends itself to photographic techniques and is therefore an inexpensive method when used in production.

1.1 REQUIREMENTS

The requirements for the microstrip antenna are given in the following table.

Frequency	5030-5090 MHz
Scan Angle	±40 degs in azimuth
Azimuth Beamwidth	2.0 degs at 5060 MHz on boresight
Azimuth Design Sidelobe	-30 dB
Elevation Pattern	0.8 to 9.0 degs uniform, 9.0 to 15.0 degs Cosecant^2, at 0 degs pattern slope should be greater than 8 dB/degree
Elevation Sidelobe	lower than -13 dB below the horizon
Power Handling	10 Watts C.W.
Beam Scan Rate	20,000 Deg/Sec.
Maximum Average Beam Step Size	0.02 Deg.
Beam Steering Accuracy	0.02 Deg.

Table 1-1 Microwave Landing System
Azimuth antenna specifications

1.2 OBJECTIVES OF THE STUDY

This study was undertaken to determine the feasibility of using a microstrip array antenna in a microwave landing system (MLS).

In this study we set out to cover the following objectives:

(i) Assess alternative microstrip antenna designs

(ii) Determine which microstrip antenna would most easily meet the requirements

(iii) Analyze the chosen microstrip antenna design

(iv) Evaluate this design experimentally

(v) Design and test short linear array

(vi) Outline a basic design for a MLS microstrip antenna

2.0 ALTERNATIVE MICROSTRIP ARRAY ANTENNAE

Broadly the microstrip array antennae can be classified in two categories:

1) resonant element arrays
2) travelling wave arrays

In this chapter a comprehensive study and analysis of existing antennae and their advantages will be carried out.

2.1 RESONANT ELEMENT ARRAYS

The common factor in resonant element arrays is that the element are resonant at or around $\frac{1}{2}\lambda$ in length. A variety of these arrays are discussed here.

2.1.1 LINEAR ARRAY OF MICROSTRIP PATCHES

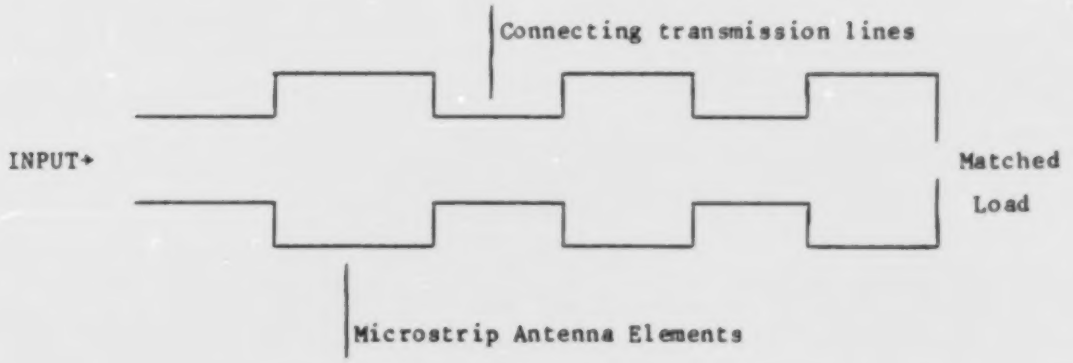

Figure 2.1 Linear Array of Microstrip Elements

This array consists of rectangular patch elements fed in series. The connecting transmission lines have high impedances so as not to disturb the electric field of the elements.

If the number of patch elements are N/2, then the array factor is given by (Ref. 3).

$$AF = \sum_{n=1}^{N} V_n e^{ik_o d_n \cos\Phi}$$

Where dn is the distance between the first and n^{th} slot. (Each patch has 2 slots of radiators and N/2 patches have N slots of radiators.)

In order to maximize the gain of the array the dimensions of the transmitting lines and radiating elements should be found by computer analysis.

In this arrangement the main beam is normal to array plane. The radiation conductance of array is given by:

$$G_{AF} = \frac{\left| \sum_{n=1}^{N} V_n \right|^2 G}{\left| V_N \right|^2 \mathrm{Re}(Y_{in})}$$

Where G is the radiation conductance of a single slot and Y_{in} is the input admittance, &

V_n = A Constant of Radiation for one slot
V_N = A Constant of Radiation for all slots

The results of some experiments carried out at 9 GHz are shown in Figs. 2.1.1-1 (Ref. 3)

A two dimensional array of above form is shown in Figure 2.1.1-2.

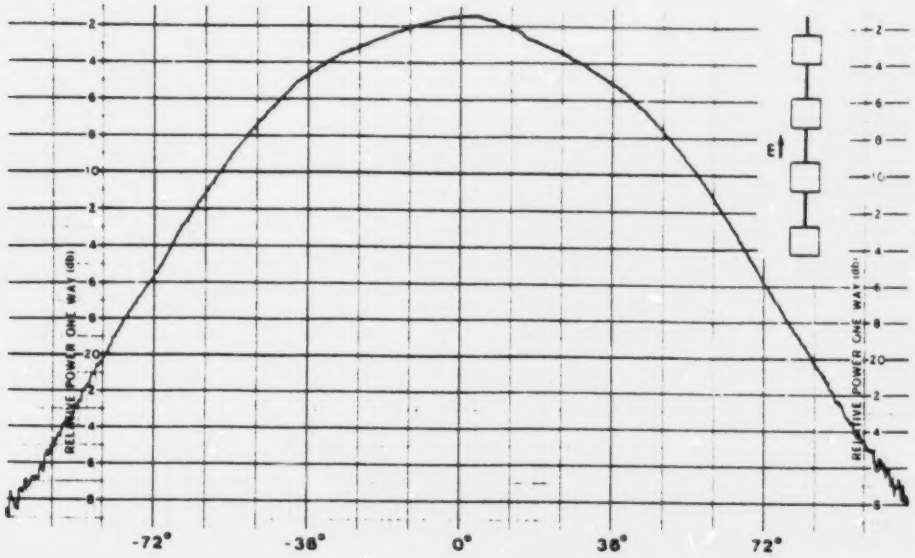

Figure 2.1.1-1a H-Plane Radiation Pattern of Four-Element Microstrip Array

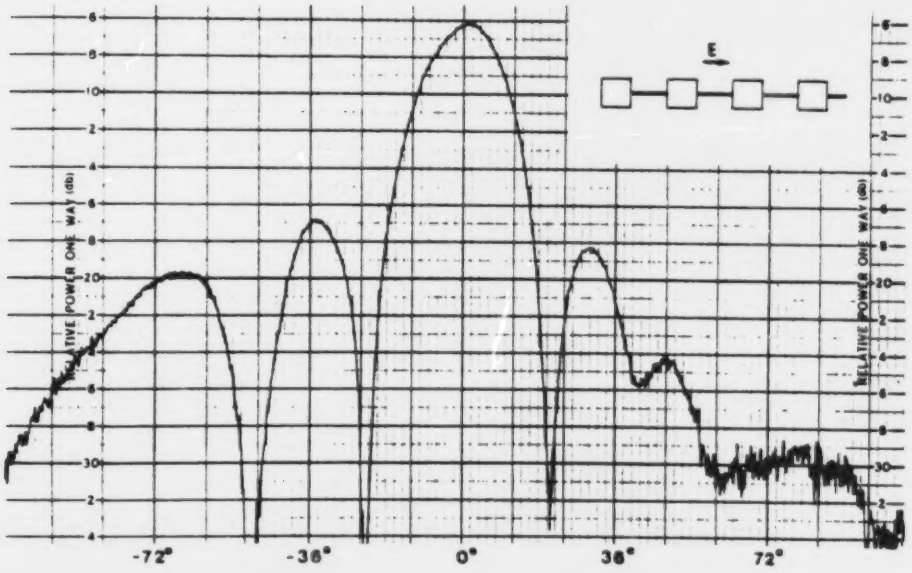

Figure 2.1.1-1b E-Plane Radiation Pattern of Four-Element Microstrip Array

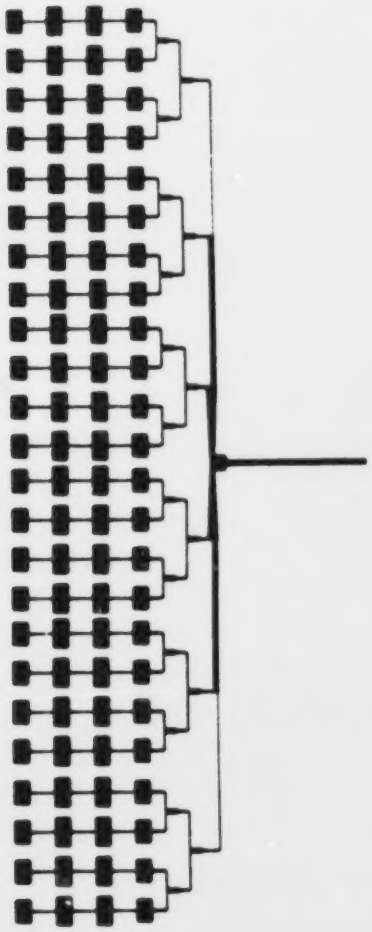

Figure 2.1.1-2 40GHz Microstrip Array Antenna
(Reprinted from Ref. 2)

This antenna array consists of 6 subarrays of 4x4 array to design a planar antenna at 40 GHz. The array had 3.5° H plane beamwidth and 26° E plane beamwidth with a 2% bandwidth over a VSWR < 2.
Fig. 2.1.1-3 shows the radiation pattern of E plane and H plane of a 4x4 sub array (Ref. 2).

2.1.2 SERIES FEEDING RESONANT ARRAY (Ref. 5)

Since an open circuit termination radiates a dipole like pattern it can be utilized as a basic radiating element. The termination can be connected to the Feeder line by a half wave length micro strip line. At resonance the radiating resistance is transferred to the Feeder line.

The relation between radiation conductance and the width of strip is shown by equation 1.2.1-5. The radiation resistance is a simple function of strip width, which suggests a simple way of controlling the output radiated power.

Consider Figure 2.1.2-1. The open circuit radiating aperture is a half wavelength from feeder line and as such the radiation resistance will effectively appear across the feeder line at the junction point. In this way the isolated half wave resonators have been attached to a feeder line. This is analogous to slotted waveguide or dielectric rod waveguide antennas.

James, et al. Ref. (5) tested a simple nine element array. The elements were spaced λg guide wave length apart (Figure 2.1.2-2 to achieve equality of phase excitation). The elements are loading the feeder line at high impedance points.

Using the relation 1.2.1-5 it is possible to adjust the width so that the radiation pattern will have specific sidelobe and beamwidth.

The theoretical analysis of series fed resonant arrays is based on transmission line theory.

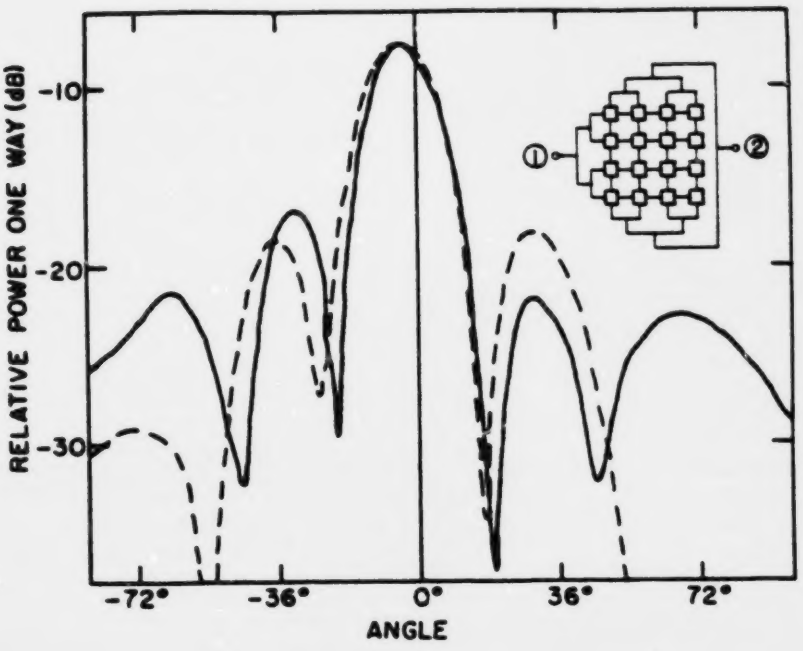

Figure 2.1.1-3 E-Plane (-) and H-Plane (—) Patterns of a 4x4 Element Microstrip Array for Port 1 Excitation
(Reprinted from Reference 2)

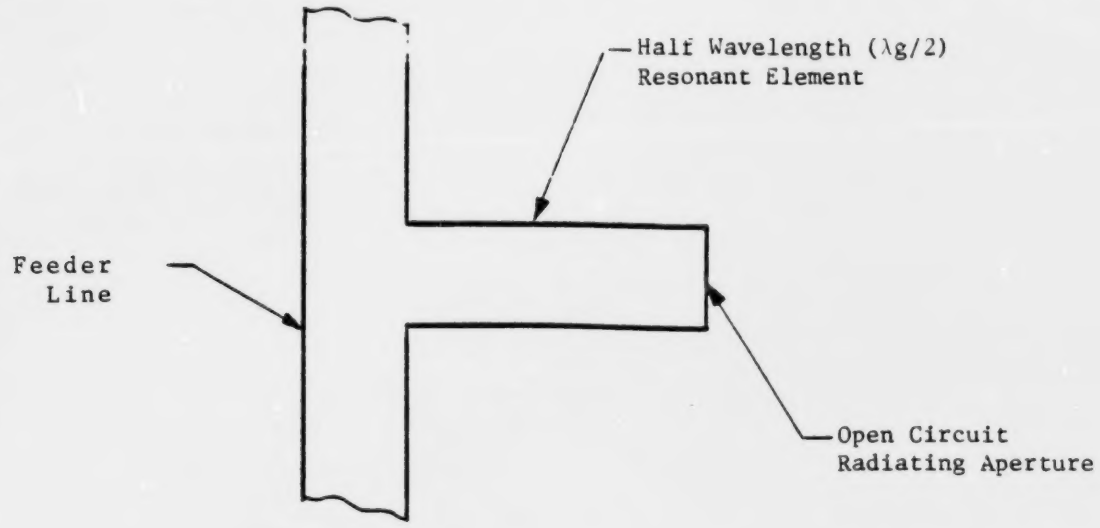

Figure 2.1.2-1 Basic Series Fed Element

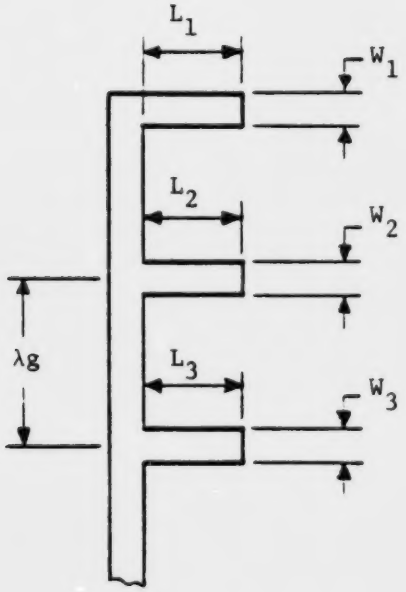

Figure 2.1.2-2 Linear Array of Series Fed Elements

As explained before the micro strip elements which are half wave length resonant stubs are connected to the feeder line and at resonance the radiation admittance is transformed directly to the feeder. Consider Fig. 2.1.2-3, which is a sketch of the feeder line. There are N stubs of radiators connected to the feeder line. Each stub has a strip width W, substrate height h and relative permittivity ε_r. A typical stub has a length L_i and its central position is D from the (i-1)th stub. The equivalent circuit of T junction involves a shunt susceptance jB_{Ti}, a transformer of ratio n_i and correction factors $d_{1,i}$ & $d_{2,i}$ The latter change the effective stub length to L_i' and the stub separation to $(D_i = D - d_{1,i} - d_{1,i-1})$. The admittance of open circuit termination of micro strip is given by $Y_{r_i} = C_{r_i} + jB_{r_i}$.

The parameters of n_i, $d_{1,i}$ & $d_{2,i}$ are given empirically by ref 5.

The i^{th} stub can be transformed to matrix form:

$$A(W_i, L_i') = \begin{bmatrix} \text{Cos h}\{(\alpha_i + j\beta_i) L_i'\} & Z_i \text{ Sin h}\{(\alpha_i + j\beta_i) L_i'\} \\ \text{Sin h}\{(\alpha_i + j\beta_i) L_i'\} \cdot Z_i & \text{Cos h}\{(\alpha_i + j\beta_i) L_i'\} \end{bmatrix}$$

$Z_i = Z_{oi} K/\beta_i$ Z_{oi} = free space line impedance

$\beta_i = 2\pi/\lambda_{gi}$ λ_{gi} = wavelength in substrate

α_i = micro strip loss

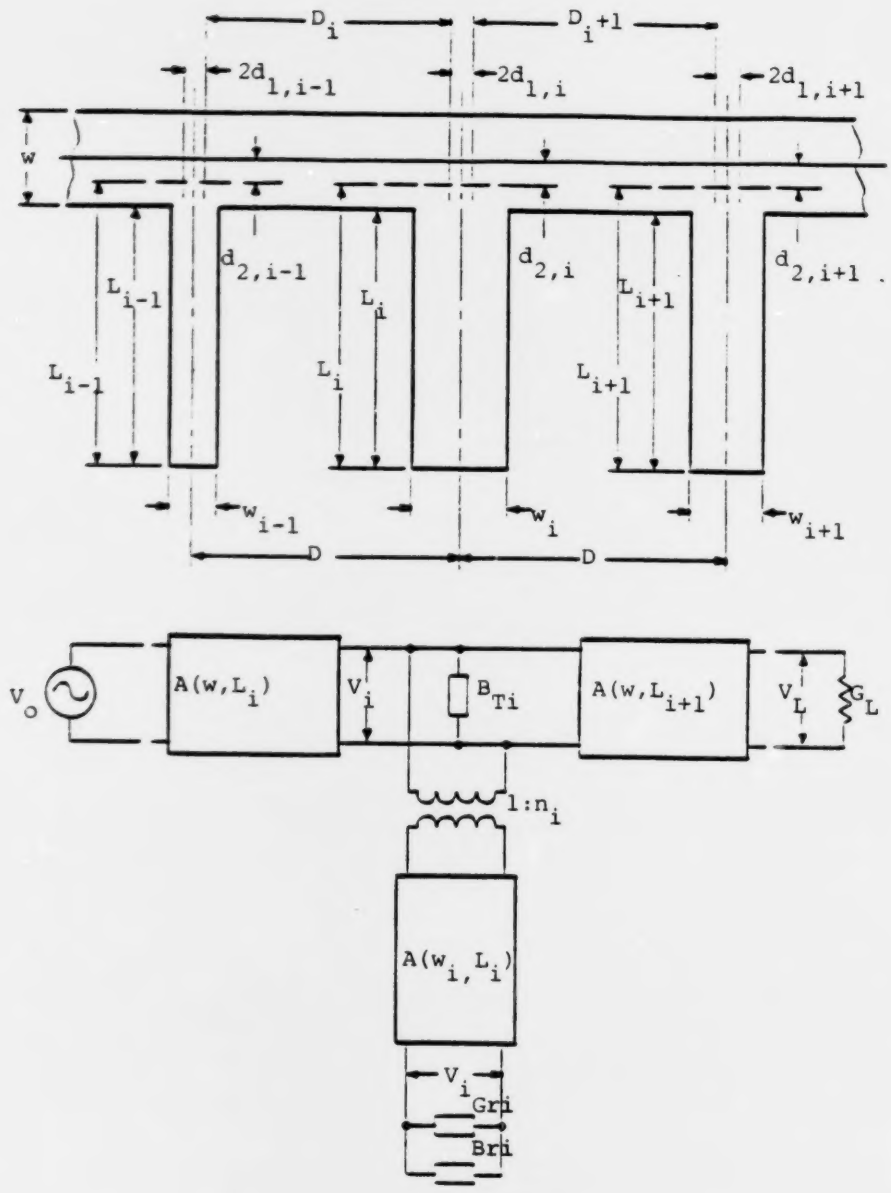

Figure 2.2.2-3 Sketch of Microstrip Feeder Showing the ith Stub and Associated Electrical Parameters

The i^{th} section of the feeder line of effective length D_i and width W can also be specified by another matrix $A(W,D_i)$. The input admittance G_o+jB_o of the entire N stub and feeder assembly can now be obtained by successive matrix-transformation. Once input parameters are determined, other parameters of the network are easy to calculate.

The authors indicate a comprehensive computer program for the network exists which calculates the radiation pattern, VSWR, etc.

In this analysis, the surface wave generated, coupling effect or radiation from T junction have not been taken into consideration.

These factors are not 2^{nd} order effects. For example Lewin in his paper (Ref. 1) indicates that the radiation from T junction account to a third of the total radiated power.

This antenna is suitable for radiation beam pointing, but not suitable to shape a radiation beam as required by MLS Antenna.

2.2 TRAVELLING WAVE ARRAYS

2.2.1 RADIATION THROUGH SLOTS IN TRAVELLING WAVE ANTENNA

Consider Fig. 2.2.1-1. This is long micro strip, and the radiation is from slots which are formed between the long edges of the micro strip and the earth plane. The geometry for the calculation of the travelling wave antenna is shown in Figure 2.2.1-2.

Slots a & b are excited by equal and opposite electric fields. These fields have constant amplitude and phase over the whole length of the slots. The slots radiate in opposite directions in a way similar to two equal and parallel magnetic currents $\overline{M}_z$, where

$$\overline{M} = \overline{E} \times n = z\, M_o\, e^{-i\beta z} \quad \& \quad M_o = \text{magnetic current at } Z=o \;\&\; M_o = 2E_o h$$

from Maxwell's equations the vector potential $\overline{F}$ is given by,

$$\overline{F} = \frac{\varepsilon}{4\Pi}\frac{1}{\eta^1}\int_o^L M(Z)\, e^{-ik(\rho_1 - Z\,\mathrm{Cos}\,\Theta)} + \frac{\varepsilon}{4\Pi}\frac{1}{\eta^2}\int_o^L M(Z)\, e^{-ik(\rho_2 - Z\,\mathrm{Cos}\,\Theta)}$$

where $\rho_1 = ((X + w/_2)^2 + Y^2 + Z^2)^{1/2} \simeq \rho_0 + x \cdot w/_2$

$$\rho_2 = ((X + w/_2)^2 + Y^2 + Z^2)^{1/2} \simeq \rho_0 + x \cdot w/_2 \qquad 2.2.1\text{-}2$$

but $X = \rho_0 \,\mathrm{Sin}\,\Theta\,\mathrm{Cos}\,\Phi$

Therefore $\rho_1 = \rho_0 + w/_2 \,\mathrm{Sin}\,\Theta\,\mathrm{Cos}\,\Phi$

$\rho_2 = \rho_0 - w/_2 \,\mathrm{Sin}\,\Theta\,\mathrm{Cos}\,\Phi$

and $$F = \frac{\varepsilon}{4\pi}\frac{e}{\rho_0}\, e^{-ikopo}\left[\int_o^L M_{(Z)}\, e^{+ik\,Z\,\mathrm{Cos}\,\Theta + \frac{w}{2}\cdot \mathrm{Sin}\,\Theta\,\mathrm{Cos}\,\Phi} + \int_o^L M(z)\, e^{ikZ\,\mathrm{Cos} - \frac{w}{2}\,\mathrm{Sin}\,\Theta\,\mathrm{Cos}\,\Phi}\right]$$

after some manipulation, we conclude that:

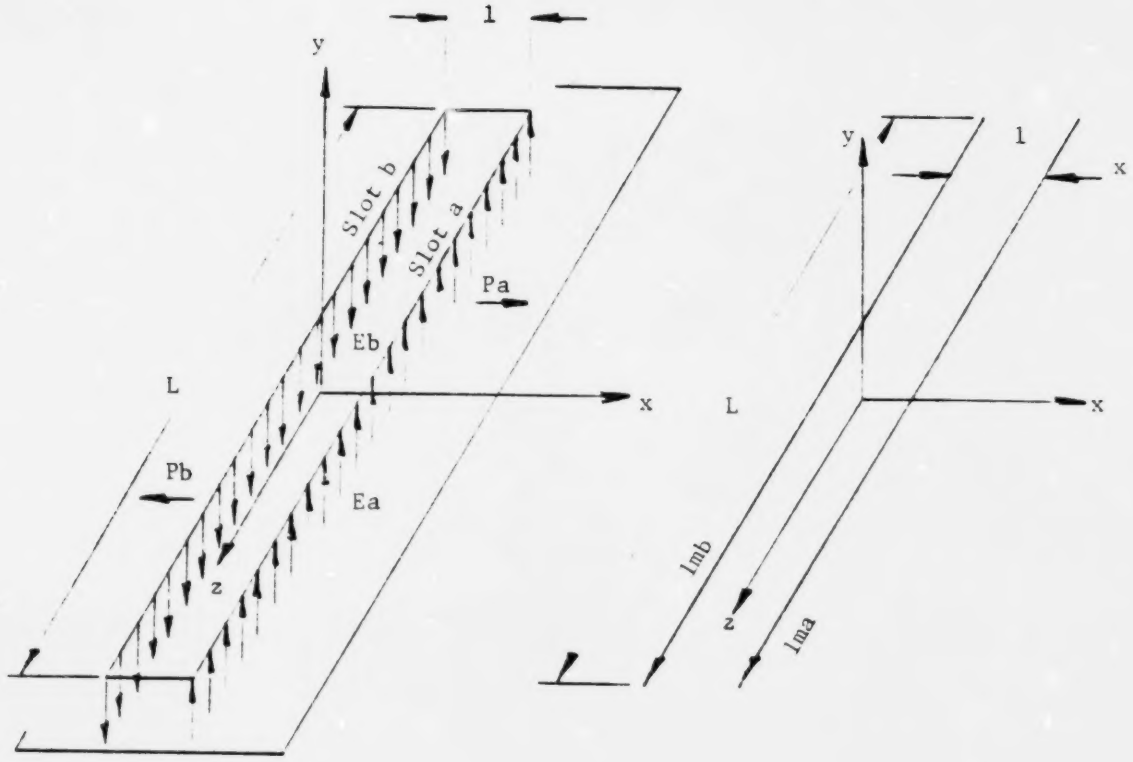

Figure 2.2.1-1
Electric Field of the Microstrip
and Equivalent Magnetic Currents

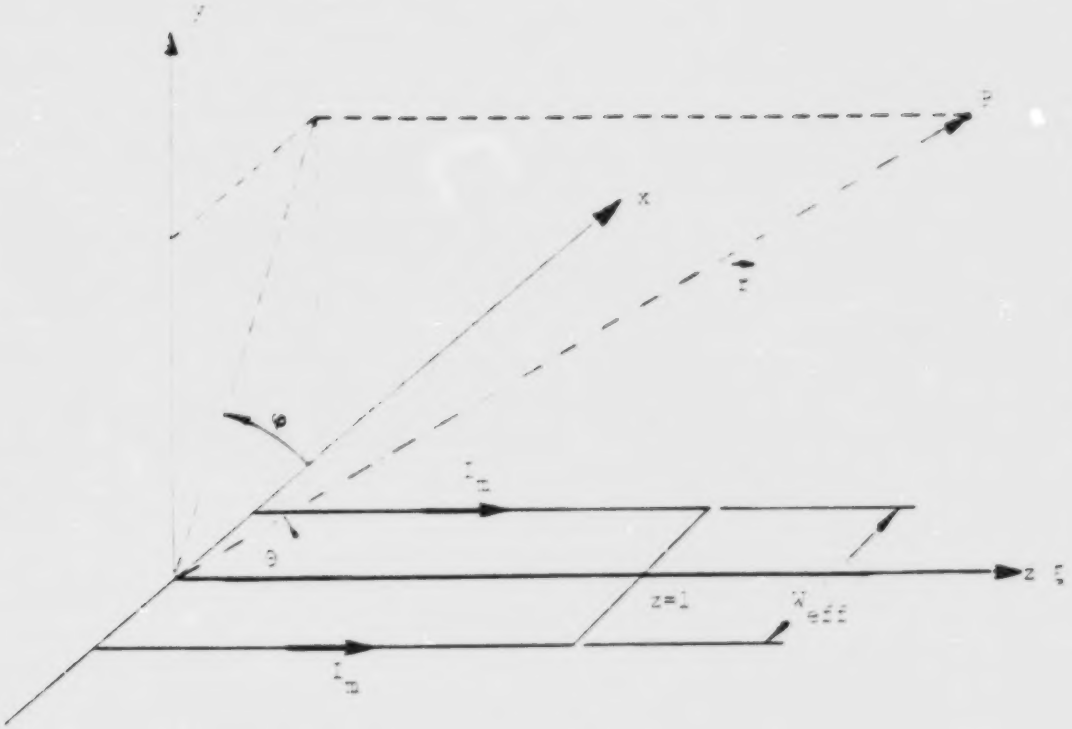

Figure 2.2.1-2

Geometry for the Calculation of
the Travelling Wave Antenna

$$E\phi = -\frac{K_0 V}{\pi}\frac{e^{-ik_0\rho_0}}{\rho_0}\left(\frac{e^{\frac{iL}{2}(k_0 \cos\theta - \beta)}}{k_0 \cos\theta - \beta}\right) \cdot \sin\theta \cos\left(k_0 \frac{W}{2} \sin\theta \cos\phi\right) \quad 2.2.1\text{-}1$$

and $E\theta = 0$

where $V = E_0 h$

The beam direction is given by:

$\theta_m = \cos^{-1} \beta/k_0$ • where β is the propogation constant in the substrate and k_0 is free space propogation constant.

The travelling wave antenna has the advantage of having a wider bandwidth. This is an important aspect of this type of antenna.

The feeding arrangement should be such as to produce constant opposite electric fields on both sides of the long radiating element. This immediately suggests a convenient length of $\lambda g/2$ between two ends of slots. Menzel, Ref (5) Suggests a feeding arrangement where a narrow quasi-TEM line feeds the radiator unsymmetrically resulting in a TEM, TEol mode conversion. He suggests an 80% conversion of incident power.

A further arrangement for feeding the long radiating element is shown at Figure (2.2.1-3) (Ref. 16).

In this arrangment the long micro strip line is fed symmetrically at N feed points. The number of inputs $N > L$
where L = the radiator length in wavelength in wavelengths
this arrangement will insure a TEM mode excitement of the radiator.

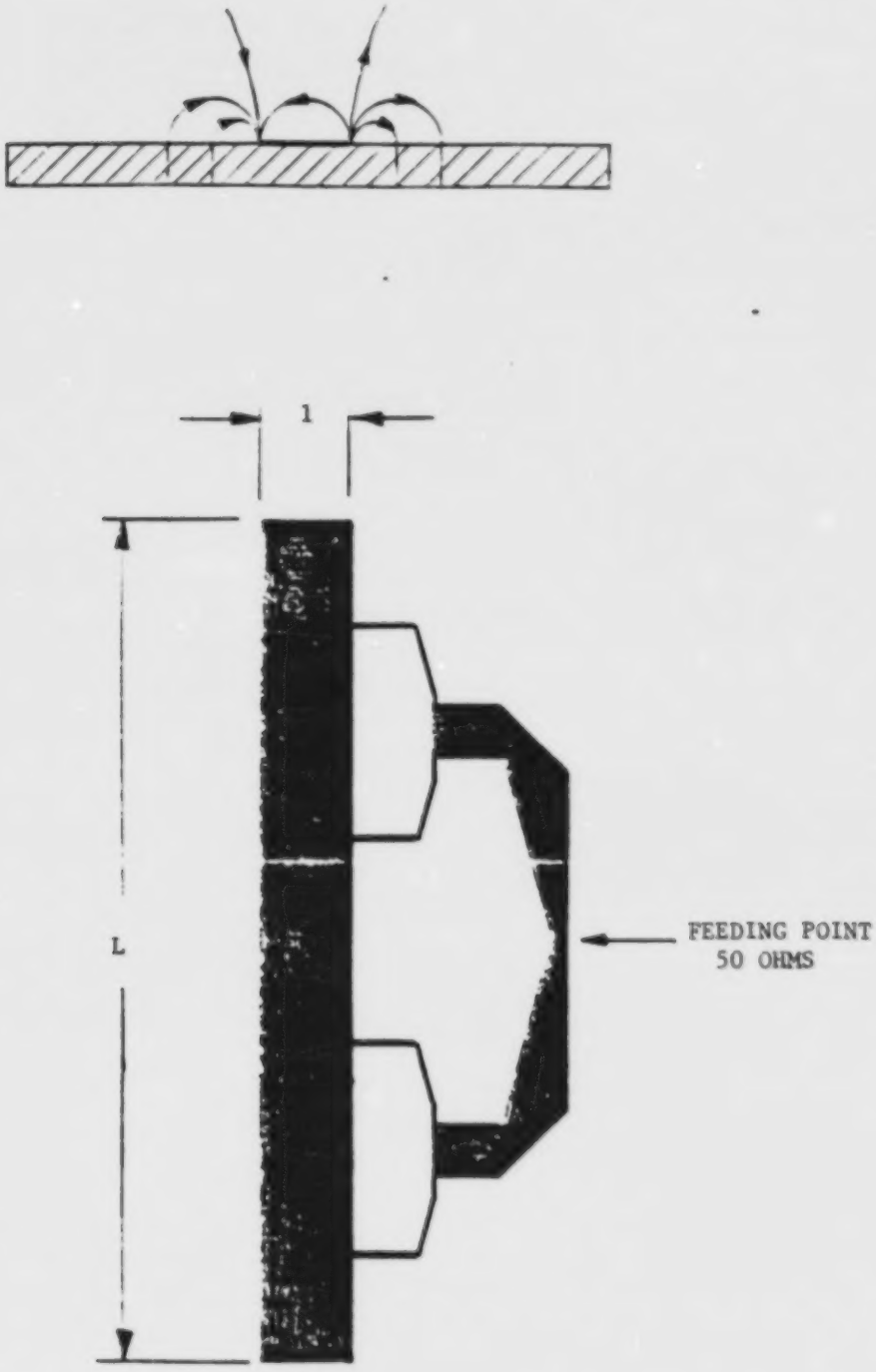

Figure 2.2.1-3 Microstrip Antenna and its Near Field
(Reference 16)

The number of feed points possible for a very long radiator is limited only by the allowable system losses that can be allocated to the feed network. The slot susceptance of such a long strip line can be considerable. This susceptance which is represented by a capacitance may be shown to be

$$C = \frac{\Delta \ell \sqrt{\varepsilon_\rho}}{cZ_o}$$

where c = velocity of light

Zo = characteristic impedance of the micro strip line

These fringe capacitances are possible to cancel by a number of short inductive stubs spread over radiating edge of the microstrip as shown in Fig. 2.2.1-4 (Ref. 16).

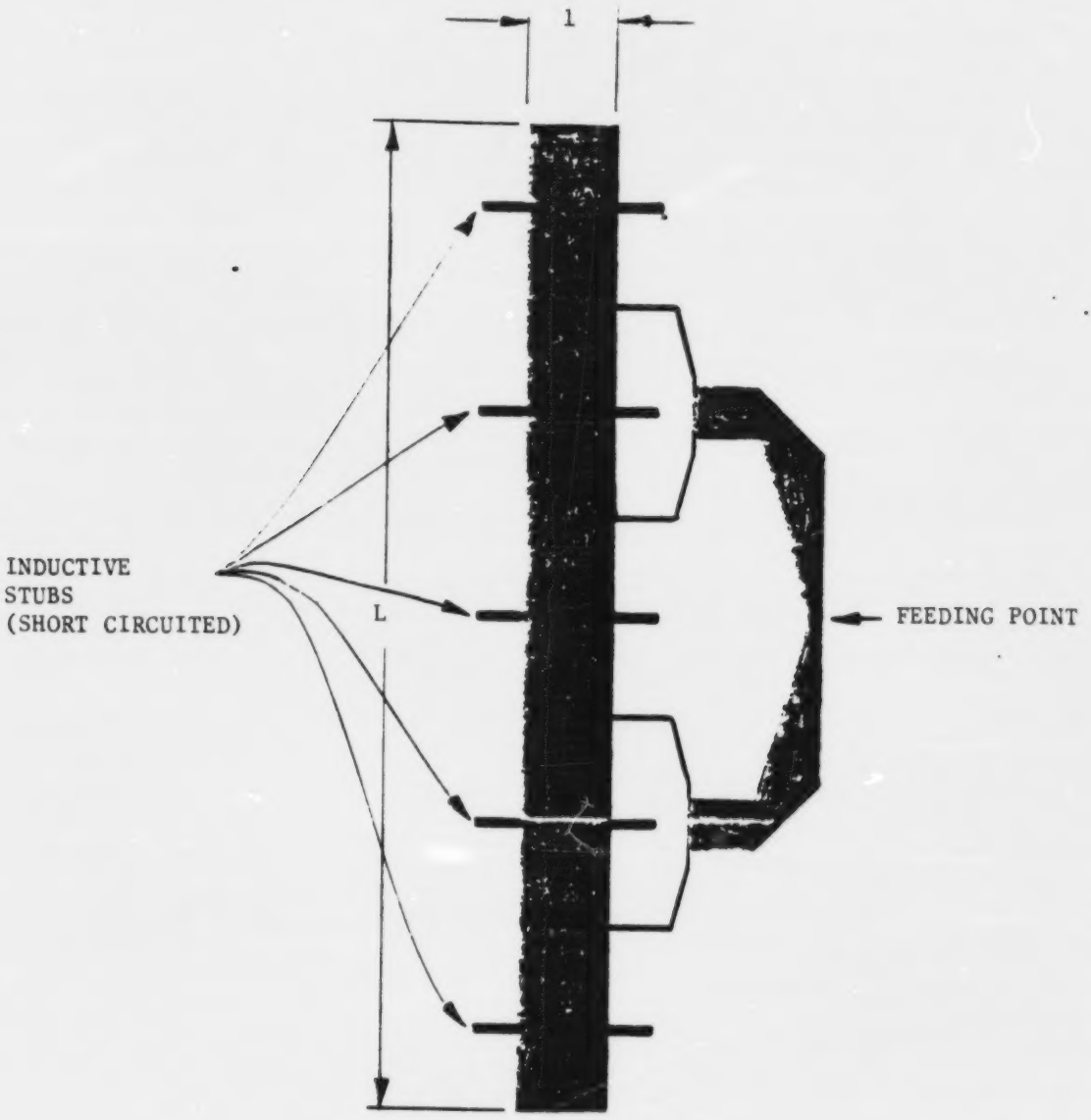

Figure 2.2.1-4 Stubs Neutralizing the Fringe Capacitance

2.2.2 FRANKLIN ANTENNA

A microstrip line backed by a ground plane is normally non-radiating but can be made to radiate by bending the corners of the micro strip line. An example of this kind of antenna is the Franklin Antenna, named after its inventor. The antenna configuration is shown in Fig. 2.2.2-1.

Franklin type antennas are basically long wire antennas with continuous, uniform cophased current distribution.

The radiation is due to pertubation of the field on zig zag section. If the wavelength is adjusted in such a way as to add up the perturbed field (like consecutive linear dipole elements spaced half wave lengths apart), there will be a stronger field on the boresight with a polarization parallel to the plane of the antenna.

A typical Franklin type micro strip line antenna is shown in Fig. 2.2.2-2. This antenna was fabricated at 9.4GHz by etching on a 0.79 mm thick rexolite 1422 copper clad board.

There are 17 straight sections in each finger of the antenna.

On the planar array, the radiators were fed in phase with equal amplitude by means of a micro strip line corporate feed system, which was printed on the same dielectric sheet as the radiators.

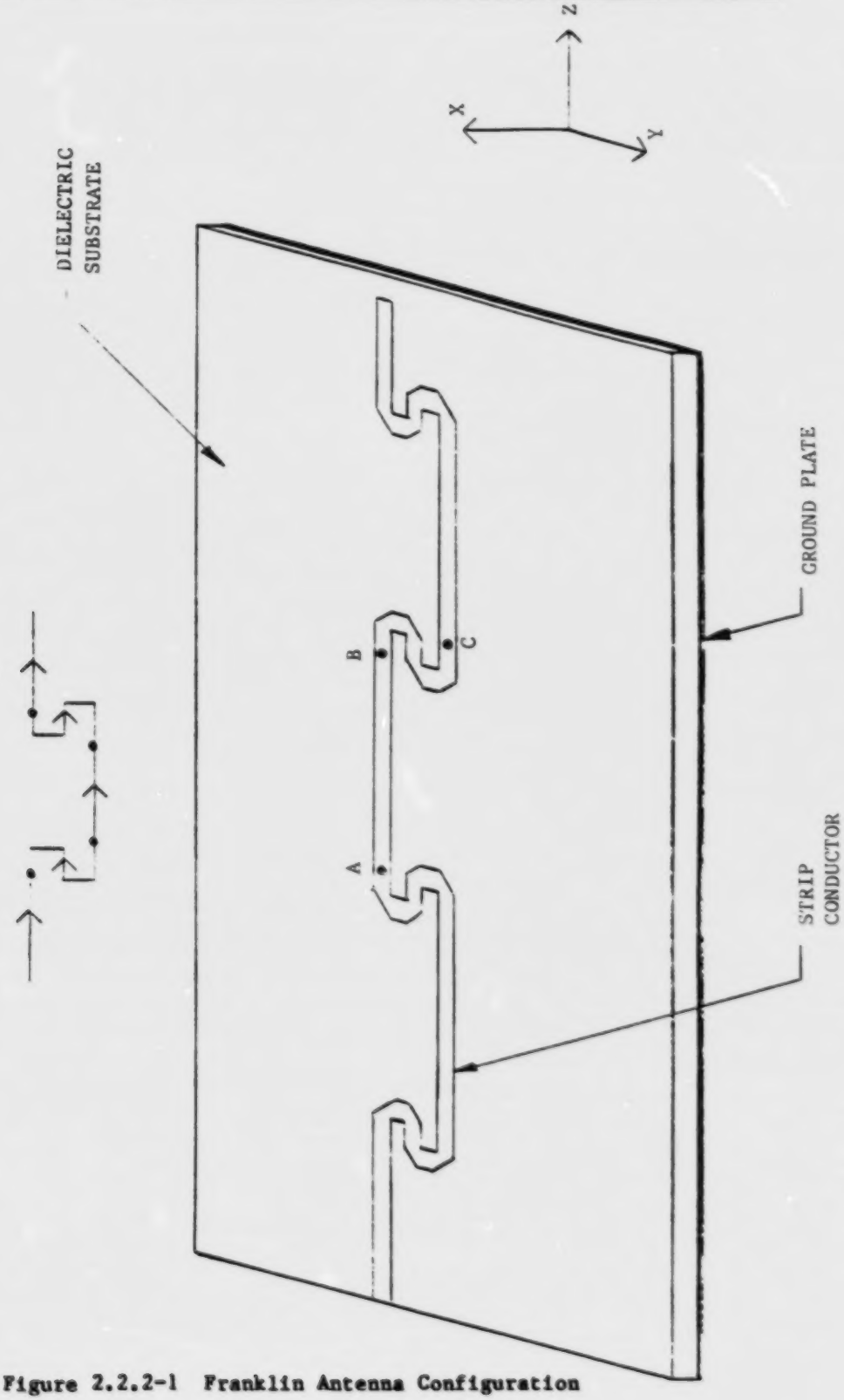

Figure 2.2.2-1 Franklin Antenna Configuration

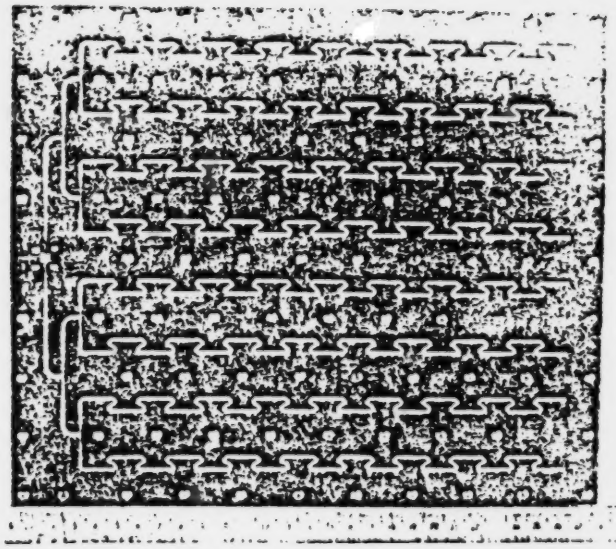

Figure 2.2.2-2 Franklin-Type Planar Array Antenna

The interval of the arrays were 28 mm and the pattern of the strip conductors are alternatively turned over in order to cancel out the component cross polarization. A gain of almost 30 db has been achieved at 9.4 GHz. Antennas of this kind, although named travelling wave antennas, have small bandwidths because of their resonant nature. A small frequency change will cumulatively change the current amplitude distribution and phase distribution progressively. Consequently, the direction of the mainbeam is frequency dependent.

2.2.3 CHAIN ANTENNA

Another configuration of travelling wave antenna is the chain antenna proposed by Tiuri et al (Ref. 7).

This antenna consists of a meandering transmission line mounted on a ground plane (Fig. 2.2.3-1).

The lines are fed in parallel from a coaxial line causing a TEM wave to propogate along the lines. The parts of the lines which are parallel to the antenna axis radiate in phase while the radiation from the perpendicular parts is cancelled due to the currents flowing in opposite directions.

The meandering lines are printed on a dielectric sheet at a distance of 0.1 wave length from the ground plane. Equal currents from the feed will flow along the meander lines attenuating due to radiation. But further along the line due to leakage of radiation, current decreases exponentially and therefore we have to assume an exponential distribution of the current.

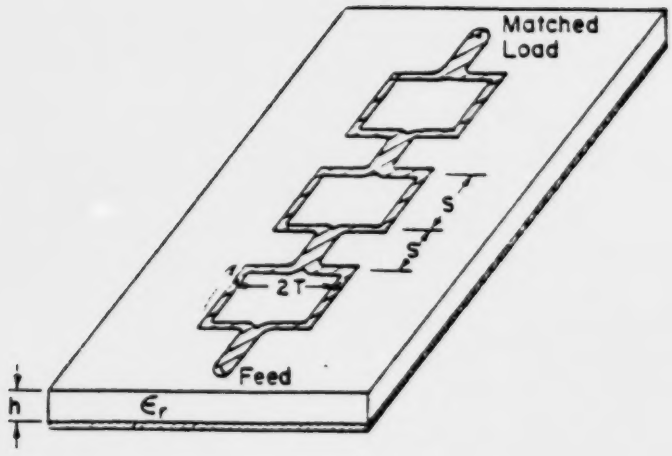

Figure 2.2.3-1 Microstrip Chain Antenna

The radiated power can be calculated by assuming an exponential current distribution and the coefficient of current distribution is obtained by the fact that the radiated power calculated by integrating over a half sphere must equal the input power minus local power.

Fig. 2.2.3-2 shows a chain antenna with 1.5 x 1.5 x .09m dimension. At 1900 MHz, it has a gain of 26 db and a beam width of 8° at bore sight.

Fig. 2.2.3-3 shows the radiation patterns at 1700 - 1900 MHz. It is possible to increase the symmetry of radiation pattern by adjusting the impedance of meander lines to have a uniform current distribution or by adjusting the distance to ground plane. Further down the line, it is possible to have a uniform power distribution. It should be mentioned that the direction of the beam is frequency dependent.

2.3 CONCLUSIONS ON ALTERNATIVE MICROSTRIP ANTENNAE

Of the microstrip antennae studied and described above, it has been decided to proceed with the rectangular patch radiator design for the MLS antenna array.

This design has been chosen for its simple shape and ease of manufacture. It can easily be represented by a transmission line model and therefore the amplitude and phase of radiation at each patch can be readily obtained. The amplitude of the radiation sources is determined by the width of the patch and the phase by their position on the line.

It should also be mentioned here that none of the antennae discussed so far have been fully analyzed mathematically, since their radiation mechanism is complex. But a physical understanding of the radiation mechanism is essential in formulating simple mathematical models for these antennae.

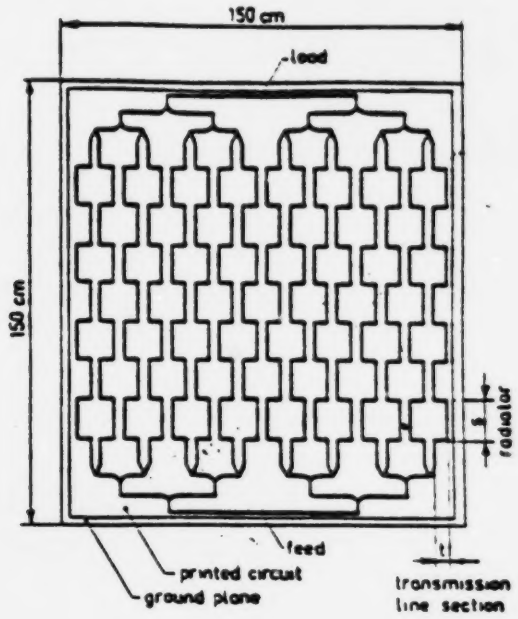

Figure 2.2.3-2 The structure of a printed circuit radio link antenna for 1.7...1.9 GHz

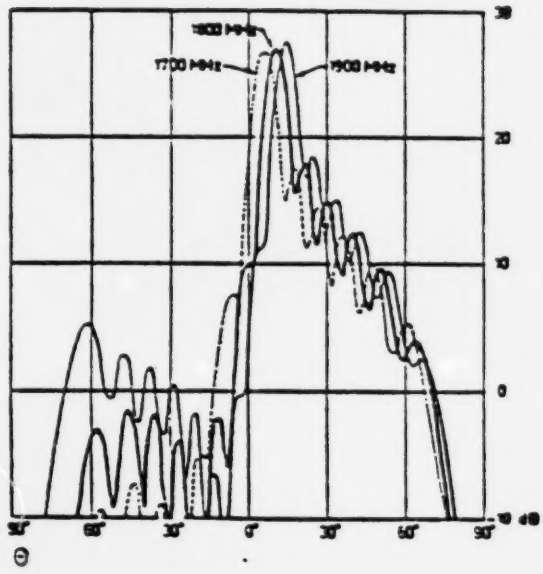

Figure 2.2.3-3 Calculated E-Plane Radiation Patterns of the Radio Link Antenna

3.0 ANALYSIS OF A RECTANGULAR PATCH RADIATOR

The radiation from a microstrip line was first analyzed by Lewin (Ref 1), in 1960. Two conductors suitably situated will create an open resonator. However, due to diffraction phenomenon, there is always leakage of energy from two open end walls. Prior to Lewin, the analyses concentrated on how to minimize this leakage. Lewin was the first to see the possibilities of utilizing this leakage as a radiation source.

3.1 APERTURE RADIATION FROM A SINGLE MICROSTRIP RECTANGULAR PATCH ELEMENT

The microstrip radiator is a conducting patch spaced a small fraction of a wavelength above a ground plane as shown in Figure 3.1-1a (Ref. 2). The fields vary along the patch as shown in Figure 3.1-1b. The radiation is from fringing fields at the open edges of the patch. They are separated by a transmission line with a very small characteristic impedance. The electric fields in these edges can be decomposed into vertical and horizontal components. Since the length of the transmission line between the slots is $\lambda/2$, the vertical component in the slots are out of phase, and the tangential components (parallel to ground plane) are in phase and add to give a maximum radiated field in a plane perpendicular to element plane. There are two basic and different approaches in analyzing the fields radiated from the open end of a microstrip line. Lewin (Ref. 1) has analyzed the slot by considering an impressed current Ip due to the polarization of dielectric material in the substrate. Once this current is known, the Hertzian vector is calculated and consequently the E_ϕ and E_θ and corresponding magnetic fields are found. This approach is very fundamental, but is only suited for far field information.

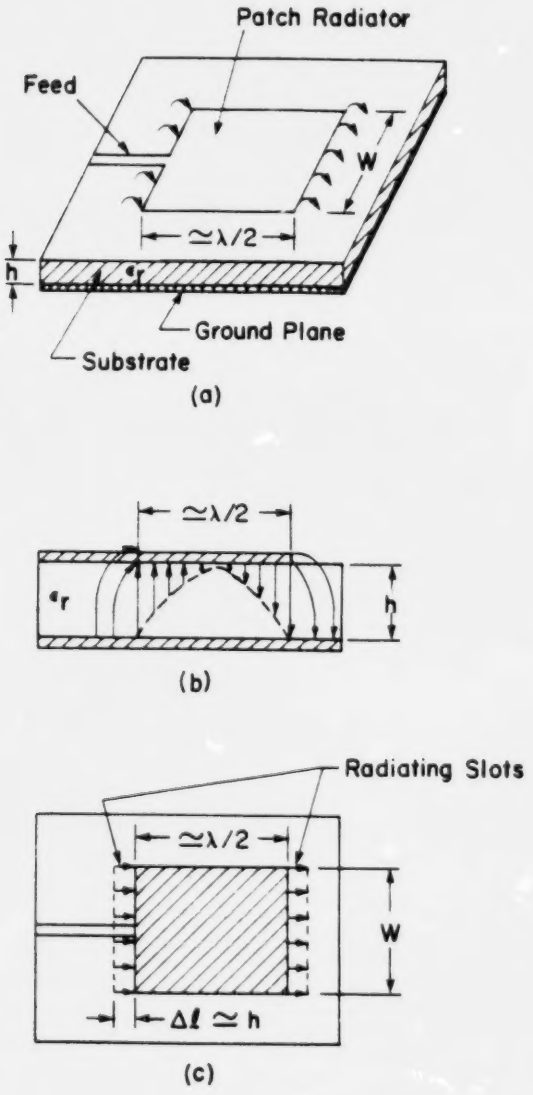

Figure 3.1-1 (a) Rectangular Microstrip Patch Antenna
(b) Side View
(c) Top View
(Reprinted from Ref. 2)

A simpler approach is to consider the slots as magnetic dipoles. The magnetic current is given by (Ref 3), Fig. 3.1-2.

$$Im = Z \cdot 2 E_x = Z \cdot \frac{2 V_o}{h} \qquad 3.1.1\text{-}1$$

where V_o = voltage across the gap of strip conductor & ground plane.

E_x = Electric Field across the gap

h = thickness of the substrate

Z = unit vector in Z direction

An approximation is made that Vo across the gap is constant.

Once the magnetic current is known, the Electric Fields can easily be found by integrating over the source point (slot area). The fields in Spherical Coordinates are given by

$$E_\phi = -i2 V_o W k_o \frac{e^{-ik_o r}}{4\pi r} \cdot F(\Theta, \phi)$$

and

$$E\theta = 0$$

$$\text{where } F(\Theta,\emptyset) = \frac{\text{Sin } (\frac{koh}{2} \text{ Sin } \Theta \text{ Cos } \phi)}{\frac{koh}{2} \text{ Sin } \Theta \text{ Cos } \phi} \cdot \frac{\text{Sin } (\frac{koW}{2} \text{ Cos } \Theta)}{\frac{koW}{2} \text{ Cos } \Theta} \cdot \text{Sin } \Theta \qquad 3.1.1\text{-}2$$

For $k_o h << 1$, the pattern expression becomes

$$E\phi = -i \frac{V_o}{\pi} \frac{e^{-ik_o r}}{r} \frac{\sin (\frac{\pi W}{\lambda} \cos \theta)}{\cos \theta} \sin \theta \qquad 3.1.1\text{-}3$$

where

h = the thickness of substrate

$k_o = 2\pi/\lambda_o$ & λ_o is free space wave length

w = width of micro strip conductor

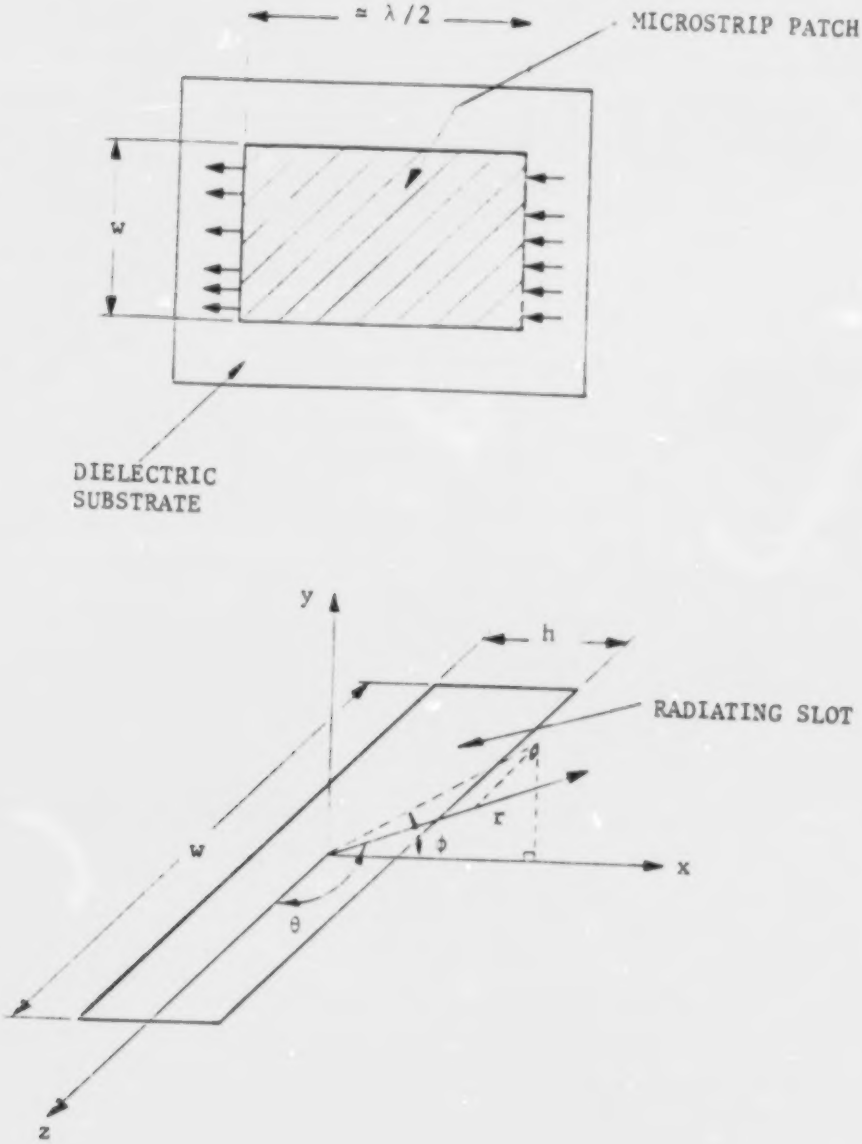

Figure 3.1-2

Microstrip Antenna Represented as Two Radiating Slots with Slot Geometry and Coordinate System

3.2 RADIATION CONDUCTANCE

In order to find the total radiated power from the slot we should integrate the real part of the pointing vector over a hemisphere of large radius. Since the slot radiates only on one side of the hemisphere, the integration is carried over half the hemisphere. Therefore the total power is given by

$$P = \tfrac{1}{2}\sqrt{\varepsilon/\mu}\ \frac{V_o^2}{\pi}\int_o^{\pi}\frac{\mathrm{Sin}^2(\pi w/\lambda o)}{\mathrm{Cos}^2\,\theta}\,\mathrm{Sin}^3\,\theta \qquad 3.2\text{-}1$$

Where $\varepsilon = \varepsilon o \varepsilon r$, the complex dielectric constant

Since Vo is the voltage across the centre of the slot a radiation conductance may be defined, as the conductance, placed across the centre of the slots which will dissipate the same power as that radiated by the slot:

$$P = \tfrac{1}{2}V_o^2 G \qquad 3.2\text{-}2$$

Where G is the radiating conductance described above

$$G = \frac{1}{\pi}\sqrt{\frac{\varepsilon}{\mu}}\int_o^{\pi}\left(\frac{\mathrm{Sin}^2(\frac{\pi W}{\lambda_o}\,\mathrm{Cos}\,\theta)}{\mathrm{Cos}^2\,\theta}\,\mathrm{Sin}^3\theta\,d\theta\right) = \frac{I}{120\cdot\pi^2} \qquad 3.2\text{-}3$$

the Integral I is solved by numerical methods (Ref 3) and a plot of $W/\lambda o$ versus G is given by Figure 3.2-1. For $W/\lambda o \ll 1$, the integration can be approximated to give

$$G = 1/90 \cdot (W/\lambda o)^2 \qquad 3.2\text{-}4$$

When $W/\lambda o \gg 1$

$$G = \frac{1}{120}\,W/\lambda o \qquad 3.2\text{-}5$$

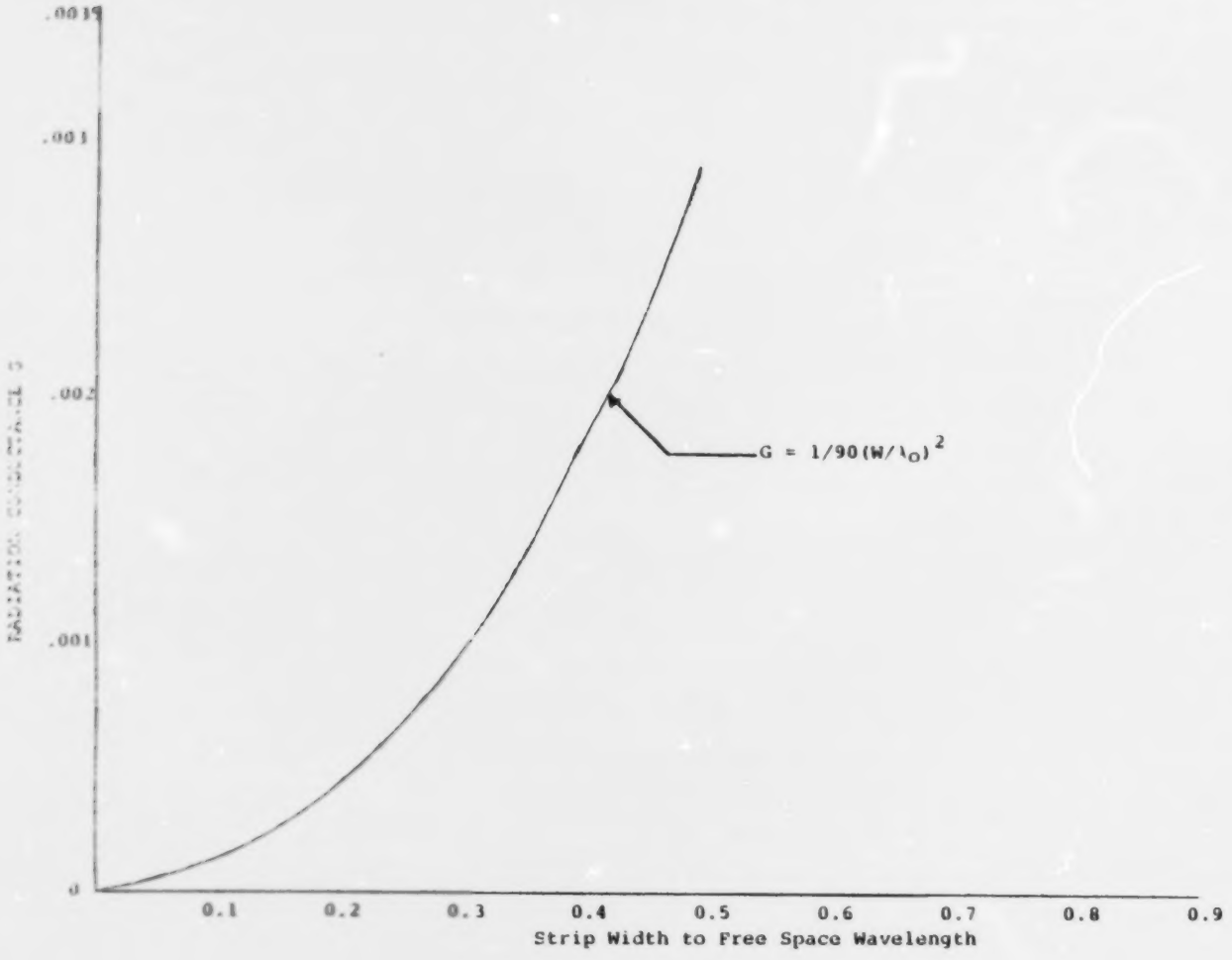

Figure 3.2-1 Strip Width versus Radiation Conductance

3.3 DIRECTIVITY

The Directivity of the slot is given by

$$D = \frac{4\pi^2 W^2}{I\lambda_o^2} \qquad 3.2\text{-}6$$

For small slots, $W << \lambda_o$, the intergral I approaches

$$I \rightarrow \frac{4}{3}\pi^2 \left(\frac{W}{\lambda_o}\right)^2$$

and D = 3 or 4.8 db, as expected for a short slot radiating into half space.

3.4 SLOT CAPACITANCE

An equivalent susceptance at the slot, represented by a Capacitor, due to the end effect is given by Hammerstad (Ref 4). He gives an approximate expression for the normalized line extension $\Delta\ell$ of an open microstrip circuit.

$$\frac{\Delta\ell}{h} = 0.412 \frac{(\varepsilon_e + 0.3)(W/h + 0.262)}{(\varepsilon_e - 0.258)(W/h + 0.813)} \qquad 3.4\text{-}1$$

where ε_e is the effective dielectric constant, and is given by

$$\varepsilon_e = \frac{\varepsilon_r + 1}{2} + \frac{\varepsilon_r - 1}{2}\left(1 + \frac{12h}{w}\right)^{-1/2} \qquad 3.4\text{-}2$$

An equivalent end capacitance can now be found,

$$C = \frac{\Delta\ell}{\nu Z_o}$$

where Zo is the characteristic impedance and ν is the phase velocity in the substrate.

3.5 EQUIVALENT NETWORK

The half wavelength resonator in Figure (3.5-1) radiates from open ends, while the radiation from the strip is negligible for wide strips. The microstrip radiating element can therefore be represented by two slots separated by a transmission line of low characteristic impedance as shown in Figure (3.5-2). The input admittance of a radiating element can be found be transforming one of the slots through the low impedance line to give:

$$Y_{in} = G + iB + Y_c \frac{G + i\,(B + Y_c \tan \beta\ell)}{Y_c - B \tan \beta\ell + iG \tan \beta\ell} \qquad 3.5\text{-}1$$

where β is the propogation constant and ℓ is the length of transmission line.

The radiating element is in resonance when the imaginary part of the input admittance cancels. This occurs when the length of the line is

$$\tan \beta\ell = \frac{2\,Y_c\,B}{G^2 + B^2 - Yc^2}$$

practical values give a resonant length slightly shorter than half a wave length. The input admittance at resonance is then

$$Y_{in} = 2\,G$$

Summary: In this section of report the important characteristics of a radiating microstrip patch, namely its Electrical fields, Directivity, Radiation Conductance, equivalent transmission line is described briefly.

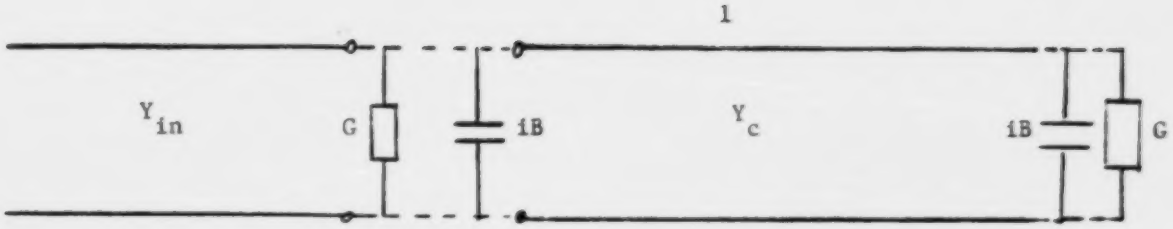

Figure 3.5-1 Equivalent Network of Microstrip Radiating Element

4.0 EXPERIMENTAL EVALUATION OF MICROSTRIP PATCH ANTENNA

4.1 MEASUREMENTS TO DETERMINE A SUITABLE COAXIAL TO MICROSTRIP TRANSITION

An important element in designing a microstrip patch radiator is coupling the power to Antenna radiator.

Power is delivered via a coaxial line to a strip line. This transition excites unwanted modes & radiates fields (space waves) in addition to the desired mode. Even if the unwanted modes (or fields) disturb the measurement to a small extent, their excitation automatically decreases the launching efficiency. The design of a proper feed is a prerequisite to good measurements. Unfortunately spurious or intentional discontinuities may set up unwanted modes and in so doing, degrade the mode purity in the whole region. There are basically two types of transition from coaxial to microstrip line.

1) Figure 4.1-1 shows the microstrip connected to coaxial line through a short post of height h. This type of launching has the advantage of

   a) the connection to microstrip is firm and solid
   b) the launching probe is totally encaved by dielectric substrate ref (1), and the launching efficiency can be improved by connecting a short circuit line

2) Figure 4.1-2 shows the common type of coaxial to microstrip transition. Figure 4.1-3 shows the coupling details and transition of radial E field-in coaxial connector to vertical E field in microstrip.

Extensive experiments were carried out to investigate the efficiency by measuring the power at the load (connected to the other end of a microstrip line) by changing the launching system. The experimental results proved the following points:

   a) common type of coaxial to microstrip transition where the coaxial pin lies horizontally in the same plane as the microstrip line (Fig. 4.1-2) is more efficient.

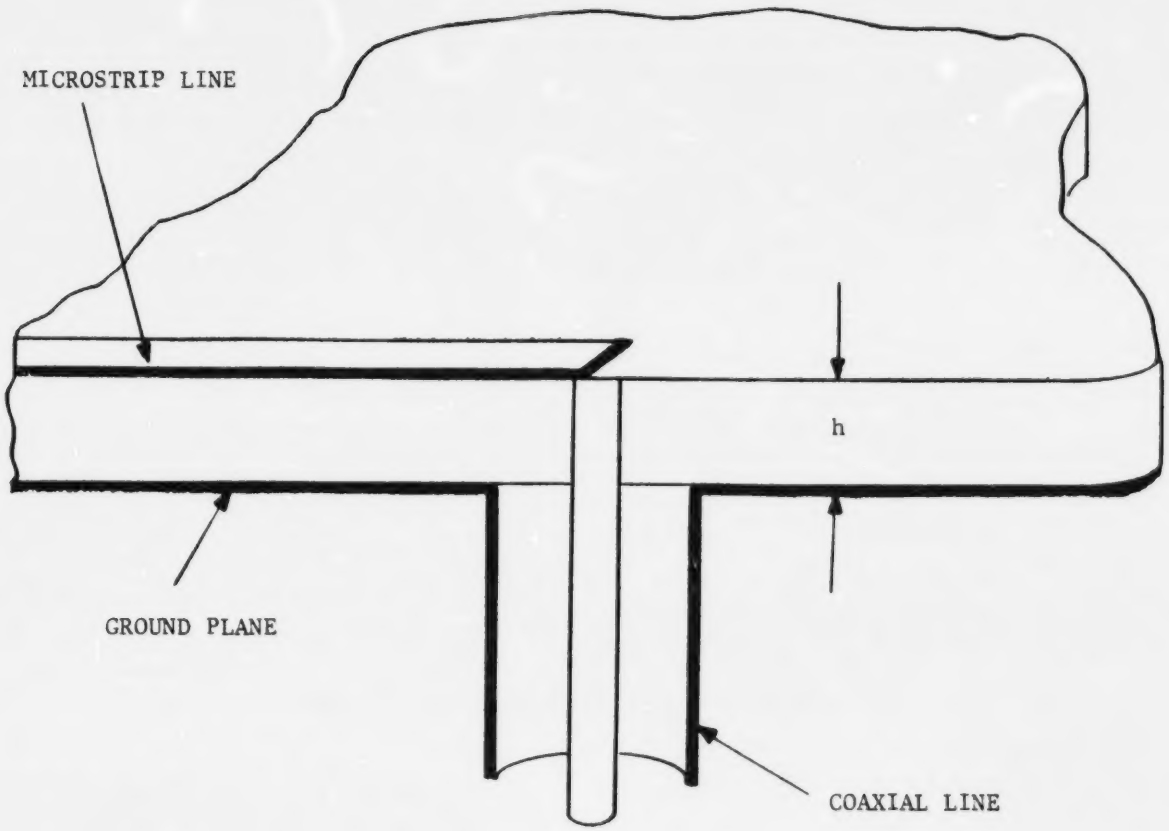

Figure 4.1-1 Coaxial to Microstrip Transition via a Short Port "h"

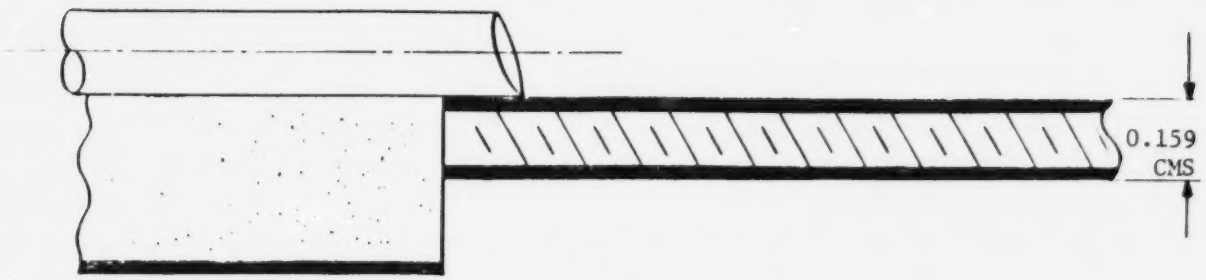

LONGITUDINAL SECTION

Figure 4.1-2 Horizontal Plane Coaxial to Microstrip Transition

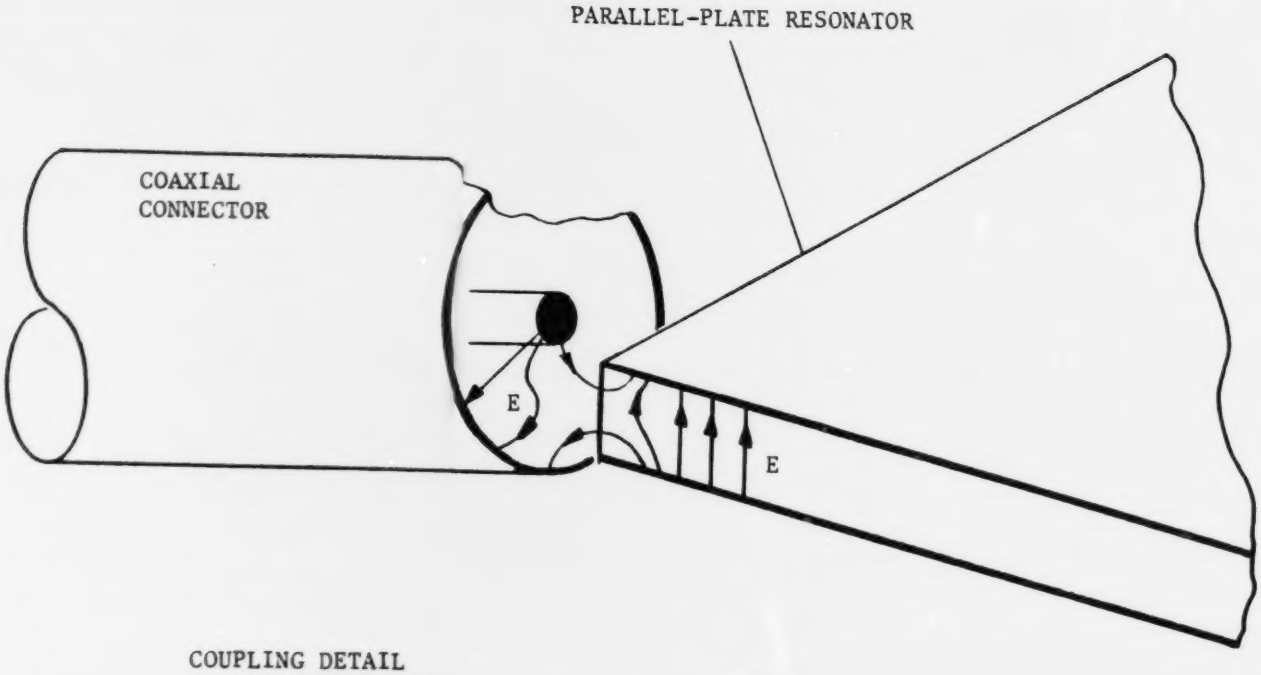

COUPLING DETAIL
(ONLY E-FIELD SHOWN)

Figure 4.1-3 Coupling Detail of Horizontal Plane Transition

b) the surface wave generated in this type of launching has smaller magnitude. This point was proven by painting the substrate with absorbing paint and observing the effect. The surface waves are the modes which have a component of Electric field in the direction of microstrip plane. The lowest order of TM (Transverse magnetic mode) has no cutoff frequency therefore it always has a small E_z Component. The launching system, shown in Fig. 4.1.1 is a more suitable method of producing the Z component of Electric Field than the method shown in Fig. 4.1.2.

4.2 INSERTION LOSS MEASUREMENTS

The experimental setup for measuring insertion loss is shown in Fig. 4.2.1. In this setup the insertion loss is measured by varying the microstrip length (L) and measuring the output power. The insertion loss is given by (Ref 8).

$$\alpha_c = \begin{cases} 1.38 \dfrac{R_s}{hZ_0} \dfrac{32-(W'/h)^2}{32+(W'/h)^2} \Lambda & (W/h < 1) \\ 6.1 \times 10^{-5} \dfrac{R_s Z_0 \varepsilon_{ef}}{h} \left[W'/h + \dfrac{0.667\, W'/h}{W'/h + 1.444} \right] \Lambda & (W/h \geq 1) \end{cases} \qquad 4.2.1.$$

where

$$\Lambda = \begin{cases} \nu + \dfrac{h}{W'} \left[1 + \dfrac{1.25\, t}{\pi W} + \dfrac{1.25}{\pi} \ln \left(\dfrac{4\pi W}{t} \right) \right] & W/h < \tfrac{1}{2}\pi \\ \nu + \dfrac{h}{W'} \left[1 - \dfrac{1.25\, t}{\pi h} + \dfrac{1.25}{\pi} \ln \left(\dfrac{2h}{t} \right) \right] & W/h > \tfrac{1}{2}\pi \end{cases}$$

$$\nu = \begin{cases} 0.5 & \text{for strip only} \\ 1.0 & \text{for microstrip} \end{cases}$$

$R_s = \sqrt{\pi f \mu_0 / \sigma}$

f = frequency

μ_0 = free space permeability

σ = conductivity of the strip conductor

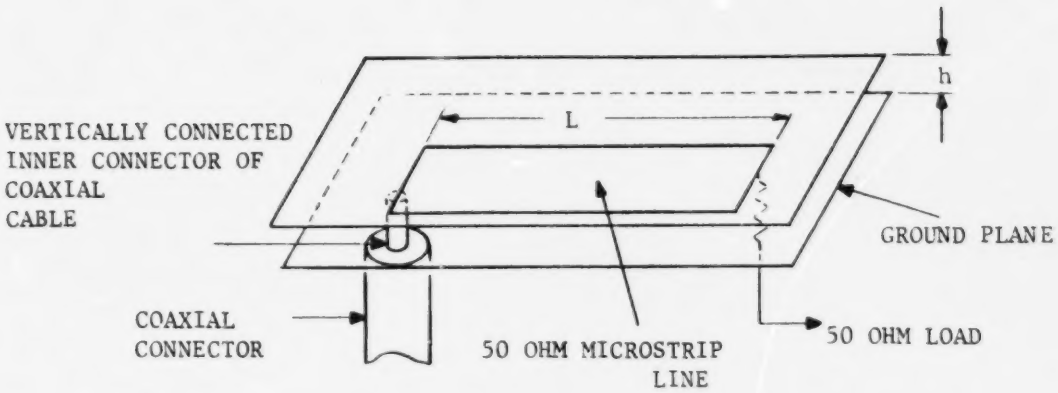

Figure 4.2-1 1. Experimental Set-up for Measuring Launching Efficiency
2. Experimental Set-up for Measuring Insertion Loss

Theoretical calculations shows that for W = 1 cms and h = 0.159 cms (Z = 28 Ω line) the insertion loss is 0.032 dB. This theoretical figure was never achieved in practice. The reason is:

1. Certain amount of energy is lost in this measurement due to radiation through microstrip line. This radiation loss because of finite width of microstrip element is an inherent part of measurement. It can be minimized by decreasing the width, but it cannot be eliminated.

2. the power launched through the coaxial transition to microstrip line is not a pure TEM mode, but a hybrid mode. The losses due to TE and TM modes (especially surface waves) also contribute to insertion loss. The experiments showed for a 50Ω microstrip line the insertion loss is 0.1 dB/wavelength, which is 50% higher than theoretical values calculated.

4.3 MEASUREMENTS OF RETURN LOSS PARAMETER OF A SINGLE RECTANGULAR PATCH

The equivalent Network of a half wave length rectangular patch radiator is shown in section 1.2.5.

It was shown when $\tan \beta l = \frac{2\ Yc\ B}{G^2+B^2-Yc^2}$, then the element is at reasonance and energy fed to it is radiated from open ends. Therefore the lower the $|S_{11}|^2$ (return loss) parameters, the higher is the radiation efficiency.

The radiation eficiency is improved by following factors:

a) a 50Ω microstrip line is connected to 50Ω coaxial launcher and by 1/4λ microstrip transformer this impedance is transferred to 128Ω and connected to centre of rectangular patch (Fig. 4.2-2). The connecting feeder line to rectangular patch should be as thin as possible so that not to disturb the radiating field from open ends.

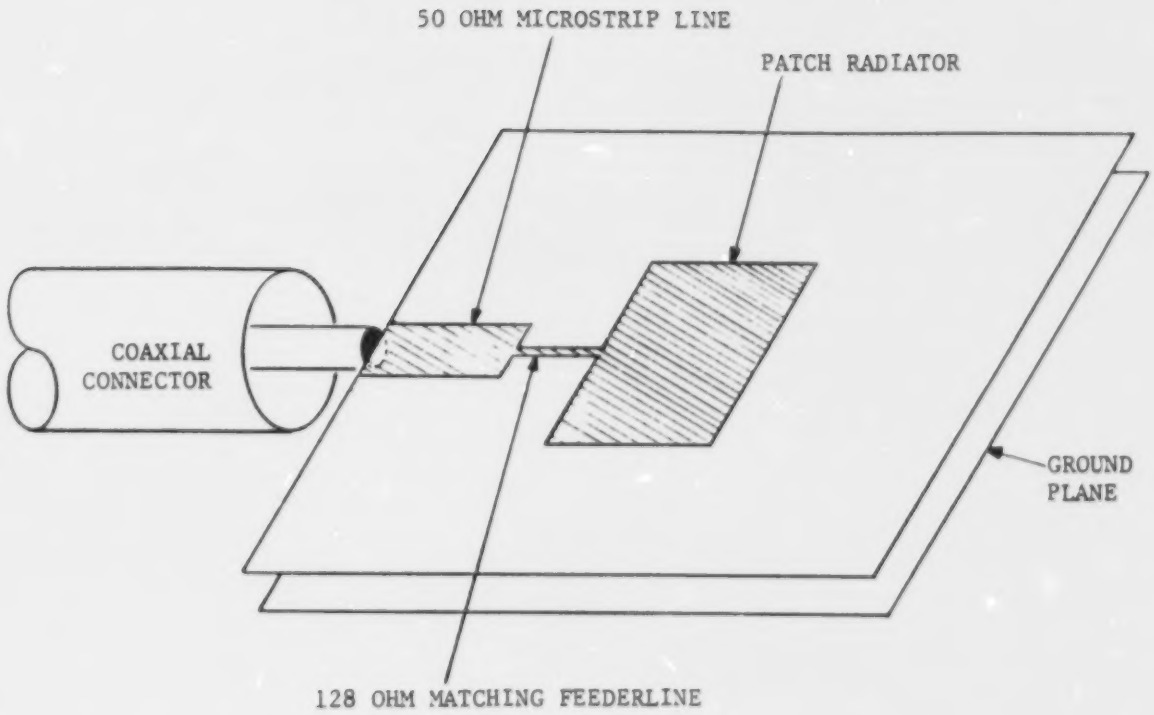

Figure 4.2-2 A Rectangular Patch Radiator with Feederlines (128Ω) and 50Ω Microstrip Transition Line

The characteristic impedances of microstrip lines are given by (ref. 9).

$$Z_m = \frac{377}{\pi\sqrt{2}\sqrt{\varepsilon_r + 1}} \left\{ \ln\left(\frac{8h}{w}\right) + \frac{1}{32}\left(\frac{w}{h}\right)^2 - \frac{1}{2}\left(\frac{\varepsilon_r - 1}{\varepsilon_r + 1}\right)\left(\ln\frac{\pi}{2} + \frac{1}{\varepsilon_r}\ln\frac{4}{\pi}\right)\right\} \Omega$$

for $w/h < 1$

$$Z_m = \frac{377}{2\sqrt{\varepsilon_r}} \left\{ \frac{w}{2h} + 0.441 + 0.082\left(\frac{\varepsilon_r - 1}{\varepsilon_r^2}\right) + \left(\frac{\varepsilon_r + 1}{2\pi\varepsilon_r}\right)\left[1.451 + \ln\left(\frac{w}{2h} + 0.94\right)\right]\right\}^{-1} \Omega$$

for $w/h > 1$

where ε_r = relative dielectric Constant of Substrate
h = substrate thickness
w = substrate width
z_m = characteristic impedance

From above relations the thickness of a 120Ω line is round to be 0.6 mm, which is a thin line and hardly disturbs the radiative field.

4.3.1 DIMENSIONS OF RECTANGULAR PATCH

The free space wave length at 5 GHz is 6 cms.
The relative dielectric constant of duroid substrate used was 2.25
λg = wavelength in substrate = $\frac{6}{\sqrt{\varepsilon_r}}$ = 4 cms. where ε_r = 2.25

The width of rectangular patch for best performance (Ref. 10) is usually W = 0.3λ where λ = free space wave length.

The radiation conductance from open ends of rectangular patch G is given by Sec. 3.2 and is

G = .001 mho

The compensation in length for capacity susceptance in open ends Δl is given in sec. 1.2.4. After deduction of 2Δl from $\lambda g/_2$, the resonant wavelength reduces to 0.465 λg.

The total input admittance of resonator is:

Y = 2G = 0.002 mho

To match this admittance to a line of 0.02 mho (50Ω impedance) a matching transformer is required. The admittance of matching transformed Y_T is given by $Y_T = \sqrt{0.002 \times .02} = 0.0063$ mho or 158.

Therefore Z_T = 158Ω where Z_T = Quarter wavelength matching impedance

In practice it was found that 128Ω impedance was providing the best match to a patch radiator.

4.4 EXPERIMENTAL RESULTS OF RETURN LOSS $|S_{11}|^2$

A rectangular patch with configurations of sec. 4.3.1 was chosen and return loss $|S_{11}|^2$ parameters were measured with a Network analyzer, where a 50Ω coaxial feeder was connected to input of the patch and a 50Ω load was connected at the output of the patch. Fig. 4.4-1 shows the return loss of a rectangular patch vs. swepth frequency bandwidth. The following points were observed in these measurements:

a. The theoretical value for half wave length resonating patch from sec. 4.3.1 was found to be 0.465 λg. In practice this value is 0.485λ. The difference can be attributed to pertubation of the field by feed points which changes the end capacitive values, hence the value of Δl.

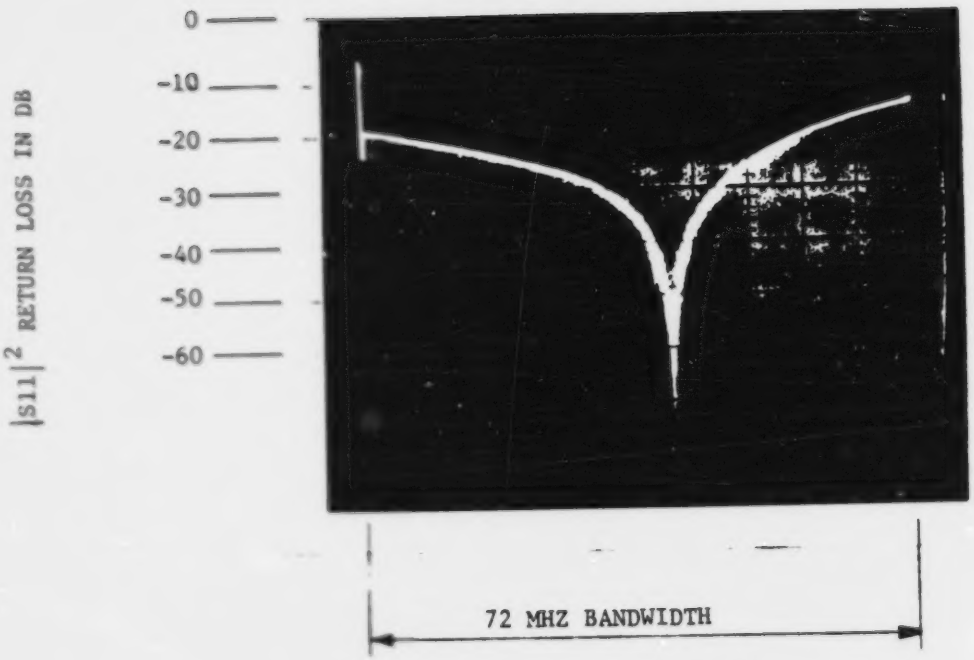

Figure 4.4-1 Return Loss Versus Swept Frequency at 5GHz

b. At resonant frequencies the return loss is usually 40 - 60 dB down. The limit of network analyzer is approximately - 40 dB. Below this value the return echo is blurred. In our measurements the return loss is below 40 dB. Therefore it was not possible to measure $|S_{11}|^2$ parameters precisely.

The VSWR (voltage standing wave ratio) is given by $VSWR = \frac{1 + |S_{11}|}{1 - |S_{11}|}$.

Therefore for -40 dB return loss, VSWR > 1.002.

By decreasing radiation efficiency it is possible to increase the bandwidth. This concept is best explained by circuit Q factor (Ref. 11). This may be defined as the ratio of the resonant frequency of the circuit and the frequency band Δf over which the power reflected is not more than one fifth (-7 dB) of that absorbed at resonant when matched, thus

$$Qt = \frac{fr}{\Delta f}$$

If a system VSWR <S is required, then the usable bandwidth of the antenna is related to the Q factors by

$$\text{bandwidth} = \frac{100\ (S-1)}{Qt\ \sqrt{S}}\ \%\ (S > 1)$$

In experiments carried out for S = 2 and Qt = 4000, the usable bandwidth was no more than 1.8%.

It was found that by increasing S (decreasing antenna efficiency) it is possible to increase the usable bandwidth.

4.5 MEASUREMENT OF $|S_{12}|$ (COUPLING PARAMETER)

In microstrip antennae a phenomena which has least been discussed in literature and which is one of most important limiting factors in array antenna design is mutual coupling between Antenna elements. The properties of isolated microstrip radiating elements are well known. In general, when a well matched individual element is placed in an array environment, its terminal properties will change as a result of mutual coupling effects. Side lobe levels may increase (and a reduction in gain), nulls may fill in or be shifted & grating lobes may appear. There is no rigorous theoretical investigation carried out in this respect. Lewin (ref 1) has investigated the mutual coupling for axial (y) & equitorial (z) separation of two radiating surfaces, but no further theoretical or experimental work (except some experiments carried out by Ref. 12) appeared in literature.

In view of importance of mutual coupling, extensive experimental work was carried out in this report.

The measurements were carried out by a Network analyzer, where port 1, of the Network analyzer was connected via 50 Ω coaxial cable to a radiating patch and port 2, (transmission) of the Network analyzer was connected via a 50 Ω detector to the second radiating patch. The distance between these patches was changed & relative transmission loss noted.

The results are shown in Figs (4.5-1) to (4.5-3).

Fig (4.5.1) shows the H plane (side by side) mutual coupling between two radiating patches.

The coupling at 1/4 wave length distance is -15 dB & decreases very rapidly to almost -38 dB at 2 wavelength distance.

Theoretically this is expected, as the Electric field is radiating from open ends in E plane, therefore it is expected that mutual coupling between two elements should be strong in E plane VS H plane. This point is confirmed by experiment.

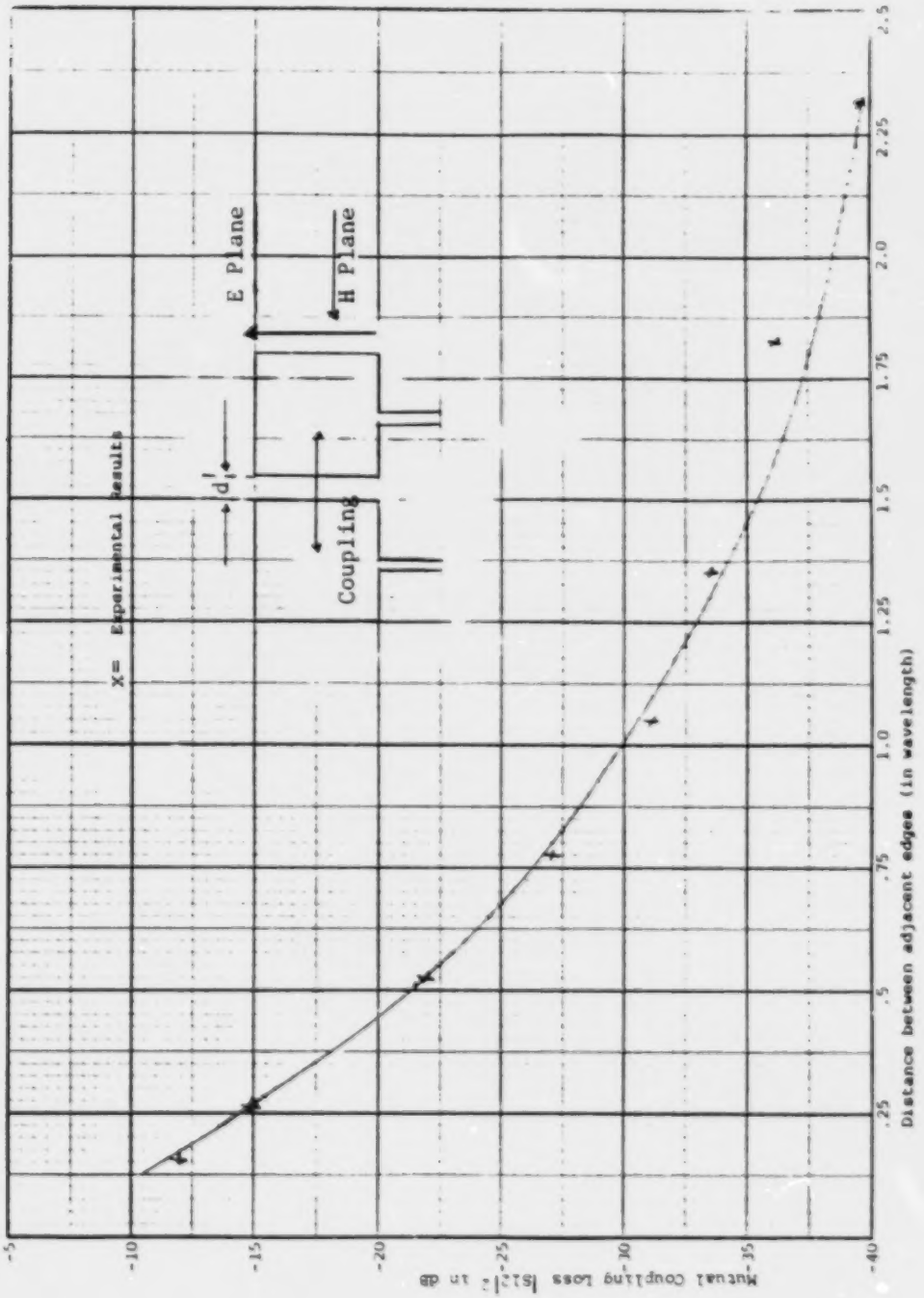

Figure 4.5-1 H Plane Coupling of 2 Rectangular Patches

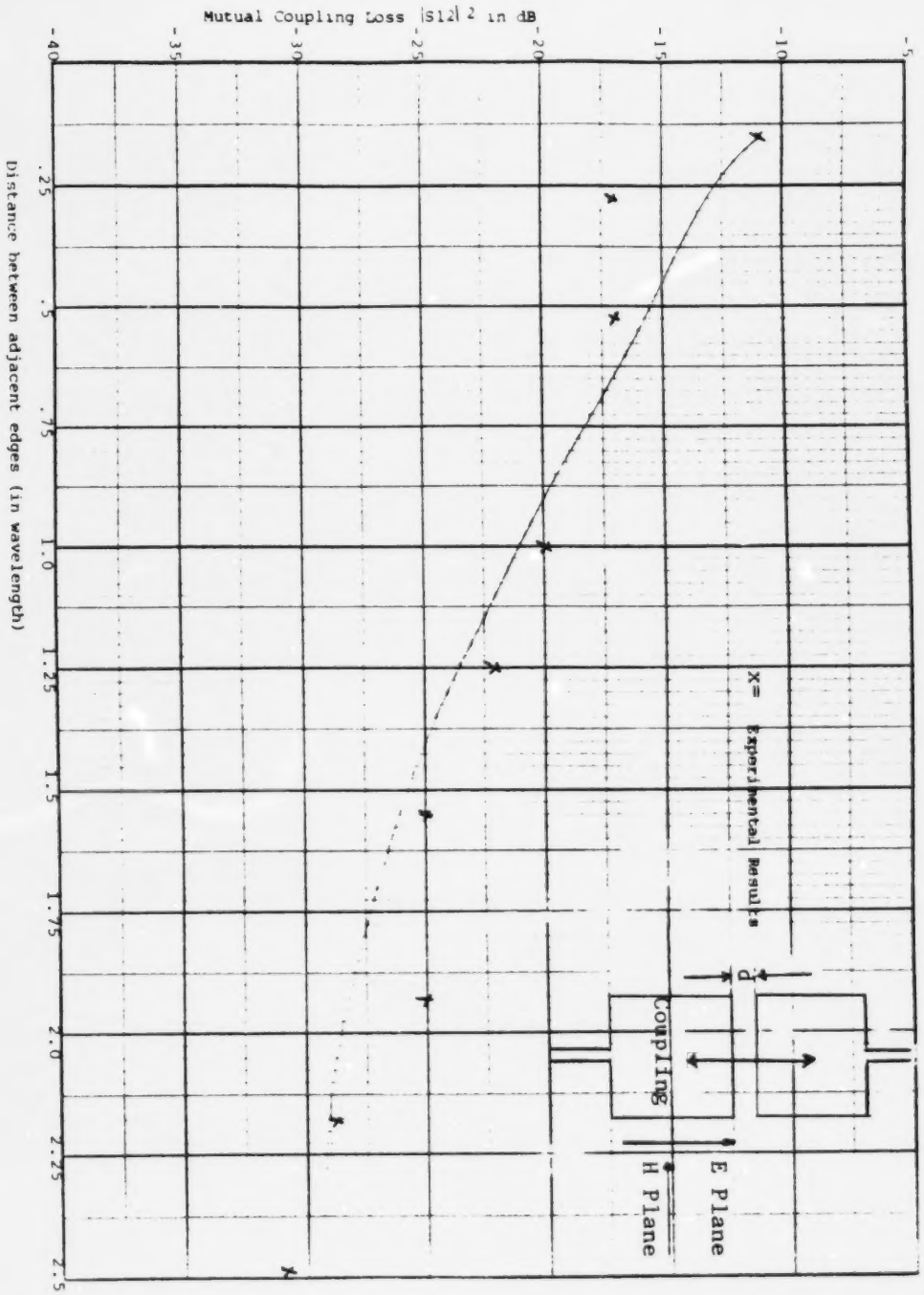

Figure 4.5-2 E Plane Coupling of 2 Rectangular Patches

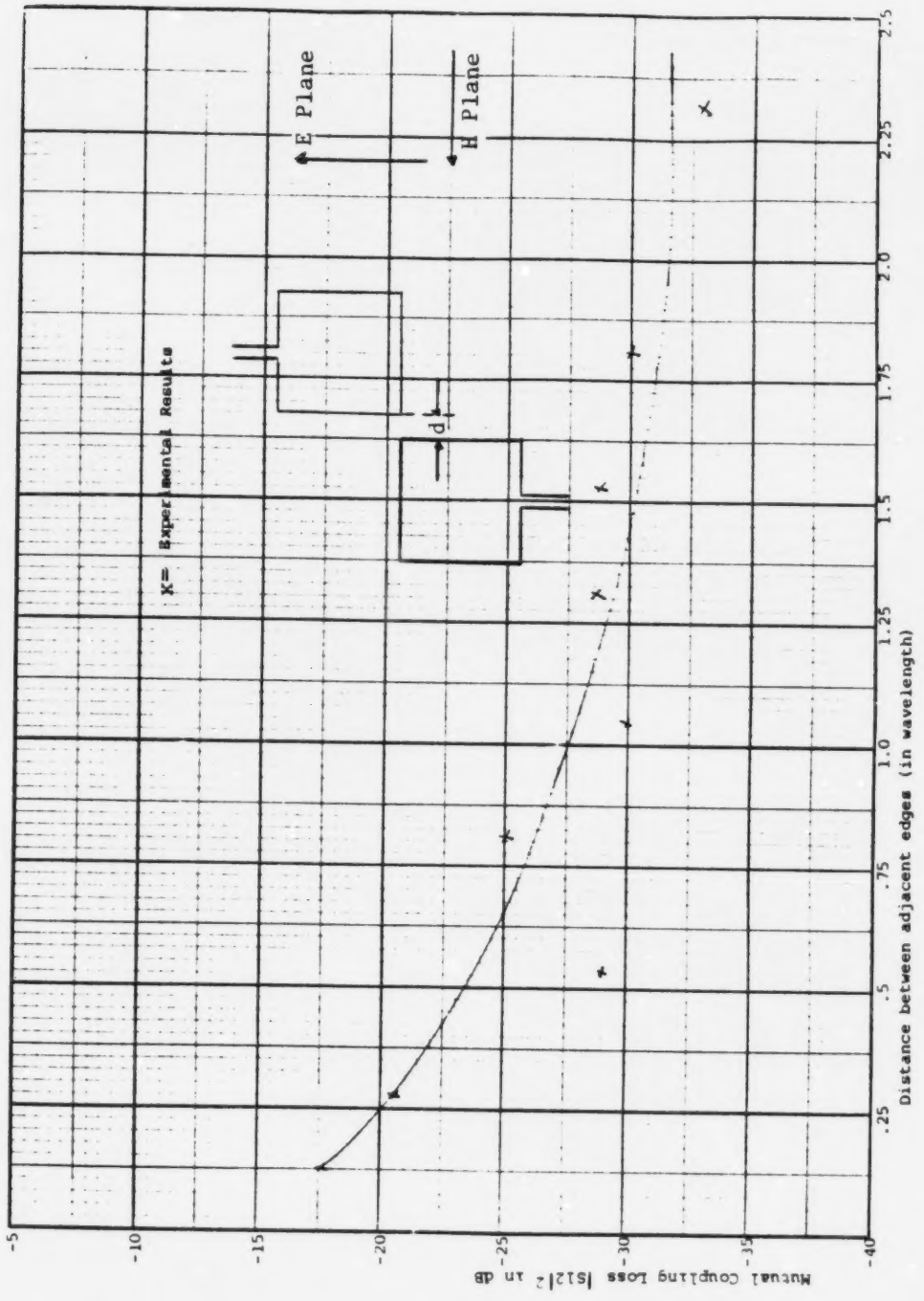

Figure 4.5-3 E Plane Side Coupling Rectangular Patches

Fig (4.5.2) shows E plane coupling of two radiating patches. It is immediately obvious that even at 2 wavelength distance the coupling is -25 dB VS -38 dB for H plane coupling. Fig (4.5.3) shows E plane side coupling between two patches. This kind of mutual coupling is between two radiating elements on either side of a feeder line. The results obtained for this type of coupling show that the values for mutual coupling lie between those obtained for H plane & E plane coupling.

In concluding this Section, the following points which are important in future investigation should be mentioned.

- A procedure is established for measuring mutual coupling parameters
- It is established that E plane Coupling is stronger than H plane coupling
- Theoretical values obtained by Lewin, in general agree with experimental values obtained, especially for H plane where they are at excellent agreement with theoretical values. Lewin gives the mutual coupling between two radiating ends in E plane, by

$$M = \frac{3}{2\alpha}(1 - 1/\alpha^2)\,\mathrm{Sin}\,\alpha + (1/2)\,\mathrm{Cos}\,\alpha$$

where M = mutual Coupling

$\alpha = 2\,\Pi/\lambda \cdot d$ where λ = free space wavelength

d = distance between two radiating ends in E plane.

In E plane coupling, the mutual coupling of two open ends of a radiating patch is found to be -14 dB, whereas by theoretical calculations it is found to be -11 dB.

The descripencies in measured and calculated values could be due to additional coupling of far end elements of radiating patches, (each patch has two radiating elements), or existence of hybrid mode which could increase the mutual coupling in E plane. These effects are more pronounced in E plan than H plane. At H plane the mutual coupling is given by:

$$M = 3\{[(1 + \alpha^2 (1 - 3/\gamma^2)/2] \sin \gamma - [1 - 3\alpha^2/2\gamma^2] \gamma \cos \gamma\}/\gamma^3$$

where

$\alpha = (2\pi/\lambda) Z$, Z is spacing between two ends of a radiating patch in E plane

$\gamma = (2\pi/\lambda)(Z^2 + Y^2)^{\frac{1}{2}}$ where y is separation of two radiating pathces in H plane.

The agreement of values obtained by above formula and by measurements are very close.

4.6 CROSS POLARIZATION MEASUREMENTS

Cross polarization is an important part of microstrip antenna design. The cross polarization is due mainly to surface wave reradiation, feed transition, radiation from T junctions, etc. The effect of a cross polarized component will be to increase the side lobe & degrade the pattern. The cross polarization effect should actually be measured in an Antenna test site, but it is possible to measure this effect with some degree of approximation with Network analyzer, by probing the field, as explained below. A sleeve dipole was made as a test probe and the gain of a patch radiator was measured at two orthotgonal planes (H and E plane) in a horizontal plane Fig 4.6.1. The difference in gain measured at E & H plane is the cross polarization, which for a rectangular patch measured was -15 dB. This figure is acceptable for low gain arrays, but for high gain arrays (-15 to -20 dBside lobe level), considerable care should be taken to minimize cross polarization by:

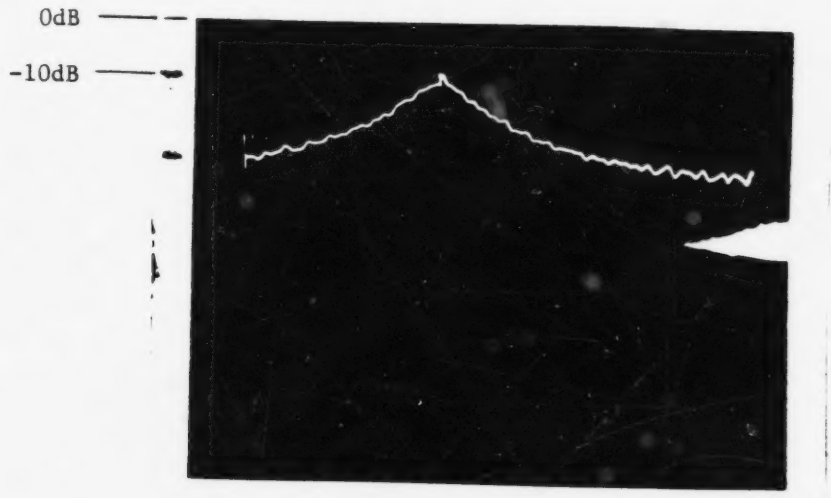

E PLANE GAIN AT HORIZONTAL PLANE

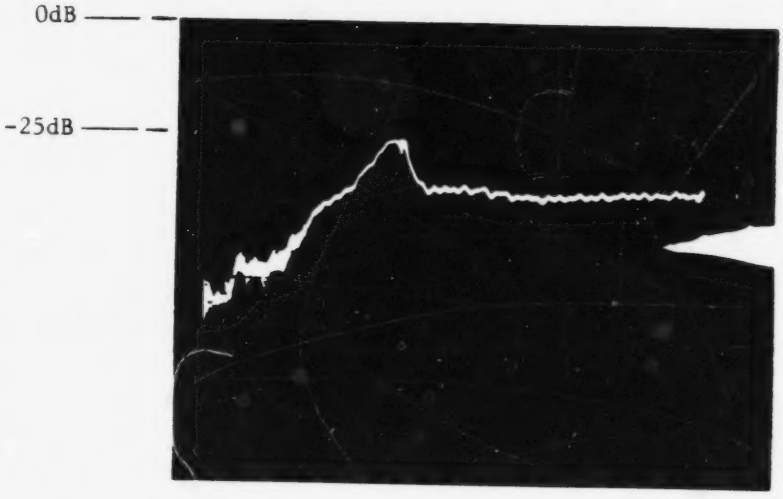

H PLANE GAIN AT HORIZONTAL PLANE

Figure 4.6-1 Cross Polarization of Eϕ Component of Electric Field at Two Orthogonal Planes

1. Reducing the surface wave radiation (by painting the discontinuties of the substrate with absorbing material)

2. By better fabrication of radiators (smooth and straight ground plane, better transition feed, constant thickness of substrate throughout the array).

5.0 4 ELEMENT SYNTHESIS OF PATCH RADIATORS

5.1 DESIGN APPROACH

As depicted in Fig (3.2-1a), the microstrip element is typically modelled as two radiating slots formed by patch edge discontinuities. The radiation conductance is calculated from the equivalent slot of width W and the susceptance is then computed from open circuit capacitance of the low impedance line. The phase shift introduced due to discontinuities is possible to find from curves (ref. 13) existing in literature. The phase shift introduced in each patch due to capacitances or inductancies of discontinuities are small, but for an array of many patches it could be considerable.

In the design of a 4 element array this effect was neglected. The array synthesis is achieved by using Tschebychev's Polynomials for 4 element patches with maximum directivity at boresight, and side lobe level of -20 dB.

The array factor (ref 14) is given by

$$(AF)_{2M} = \sum_{n=1}^{2} a_n \operatorname{Cos}\left[(2n-1)u\right] = a_1 \operatorname{Cos} u + a_2 \operatorname{Cos} 3u \qquad (5.1)$$

where

AF = array factor

$u = \pi d/\lambda \cdot \operatorname{Cos} \theta$, θ is the angle from horizon. At boresight $\theta = 90^\circ$

a_n = Tschebychev's polynomials

For a side lobe level = -20 dB, the power distribution in 4 elements array from relation 5.1 is given by:

Elements,	1	2	3	4
power	0.224	1	1	0.224

For 4 element series array, total power including 10% power wasted in a 50 Ω load is 2.7.

Therefore the percentage of power in each element is given by:

	Fraction of power in each radiator		Power delivered to Next Element
1.	$\frac{0.224}{2.7} = .083$	———	2.7 - 2.7 x .083 = 2.48
2.	$\frac{1}{2.48} = .403$	———	2.48 - 2.48 x .403 = 1.48
3.	$\frac{1}{1.48} = .676$	———	1.48 - .676 x 1.48 = .48
4.	$\frac{.224}{.48} = .467$	———	.48 - .48 x .467 = .26

From relation (1.2.1.5) the power is related to patch width (power)$^{\frac{1}{2}}$ a width of radiating element for a 2 cm patch size (maximum dimension), the 4 element array dimensions are,

	Element Size	Power radiated %
element No. 1	0.236	8.3
	1.21	40.3
Normalized to this value	2.0	67.6
	1.44	46.7

Some attempts were made to measure the near field and then extrapolate the far field, but it was not possible to measure the phase and amplitude correctly and further attempts were abandoned.

6.0 MLS MICROSTRIP ANTENNA - BASIC DESIGN CONCEPTS

The MLS azimuth antenna will have an aperture within 80 inches x 40 inches (2032mm x 1219mm) as shown in Figure 6.0-1. The azimuth antenna will consist of 54 microstrip linear arrays in the vertical plane with each array having 32 radiating elements.

A corporate feed will be used to supply the 54 linear arrays with an amplitude distribution as in a Taylor distribution to provide the appropriate azimuth beam pattern.

The elevation pattern will be shaped by the 32 rectangular patch elements in each linear array.

6.1 PATTERN SYNTHESIS

The elevation pattern required to be produced by the microstrip array is given in Table 1-1.

Shaping the elevation pattern will be achieved by optimizing the width and position of the patch elements along the linear array to give the required amplitude and phase distribution across the aperture. The amplitude of excitation is governed by the width of the patch and the phase by its position along the line.

The required amplitude and phase distribution across the aperture is obtained from computer synthesis techniques on the required far-field radiation pattern. These synthesis techniques have been used extensively at CAL for various types of antennas.

6.2 PATCH ELEMENT CHARACTERISTICS

Once the amplitude and phase distribution that the radiators have to achieve has been determined, the width of the patch and its position along the line can be found by considering the equivalent network of the array (Figure 6.2-1).

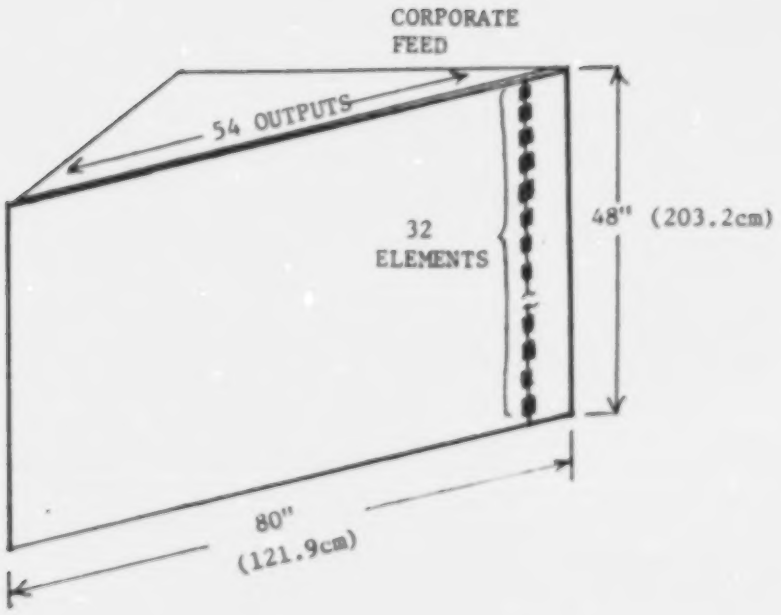

Figure 6.0-1 MLS Azimuth Antenna

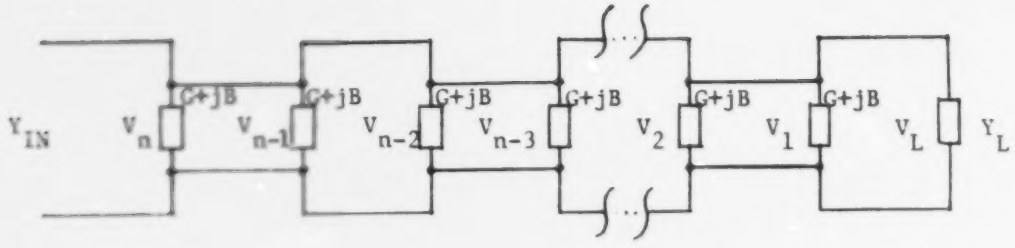

Figure 6.2-1 Equivalent Network of Linear Patch Array

The characteristics and performance of a single rectangular patch is described in detail in Section 3.

Equation 3.2-2 gives the power radiated by one edge of the patch radiator as:

$$P = \tfrac{1}{2} V_o^2 G \qquad 6.2\text{-}1$$

where V_o is the voltage at the edge of the patch
and G is the radiation conductance

Using the amplitude distribution and the equivalent network of the array, the conductance of the patch can be found from equation 6.2-1. The width of the patch is then determined by equation 3.2-4, namely,

$$G = \frac{1}{90} \left(\frac{W}{\lambda_o}\right)^2 \qquad 6.2\text{-}2$$

An expected maximum width for a patch radiator is given by (Ref. 10)

$$W = \frac{c}{2f_r} \left(\frac{\varepsilon_r + 1}{2}\right)^{-\frac{1}{2}} \qquad 6.2\text{-}3$$

which is the practical width for an efficient radiator on a dielectric substrate of thickness h and an antenna operating frequency of fr, c is the velocity of light. For the case of an operating frequency of 5.06 GHz and a dielectric constant ε_r of 2.55

$$W_{max} = 22.25\text{mm}$$

which is 0.4 times the free space wavelength or 0.6 times the guide wavelength.

The length for a resonant patch is given by (Ref. 10)

$$L = \frac{c}{2f_r \sqrt{\varepsilon_e}} - 2\Delta\ell \qquad 6.2\text{-}4$$

where $\Delta\ell$ and ε_e are given by equations 3.4-1 and 3.4-2. For this case, L = 17.83mm.

6.3 ANTENNA PERFORMANCE

Using the design procedure outlined above, it is expected to be able to build a linear array of 32 rectangular microstrip radiators which will provide the following characteristics:

Radiation Efficiency	:	≅ 70%
VSWR	:	better than 1.2
Return Loss	:	better than -20dB
Microstrip Losses	:	≅ 1.1 dB
Power Lost in Load	:	≅ 0.3 dB

It has already been shown that it is possible to produce a microstrip array which will meet the requirements of an MLS shaped elevation pattern using a design procedure similar to that outlined above (Ref. 15). The radiation patterns obtained are shown in Figure 6.3-1.

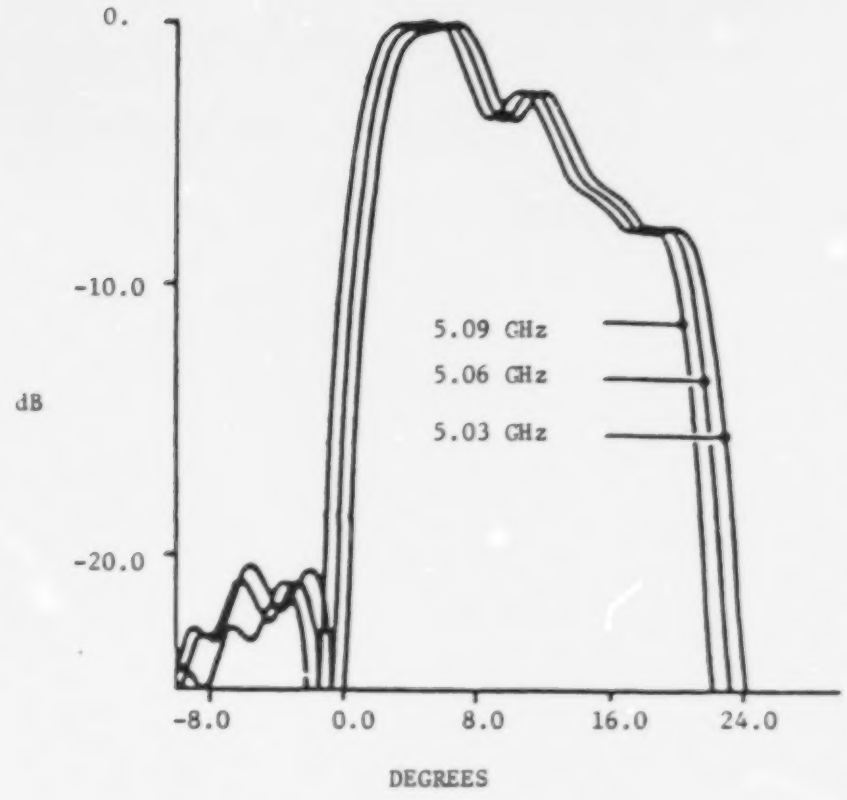

Figure 6.3-1 Radiation Pattern for 32 Element Patch Array
(Reference 15)

7.0 CONCLUSIONS

The objectives of this study were to:

(i) Assess alternative microstrip antenna designs,
(ii) Determine which design would most easily meet the requirements,
(iii) Analyze the chosen antenna design,
(iv) Evaluate the design experimentally,
(v) Design and test a short linear array,
(vi) Outline a basic design for the MLS microstrip antenna.

In assessing alternative microstrip designs, a linear array of rectangular patch radiators was chosen as the best candidate for the MLS antenna. The patch array antenna proved easy to design and manufacture, provides the correct polarization, good gain and VSWR.

A detailed analysis of the chosen design is given in Section 3 covering the important aspects of the patch characteristics.

Rectangular patch antennas were made and experimental measurements made of their characteristics such as insertion loss, return loss, mutual coupling and cross-polarization. It was shown that Lewin's theoretical calculation for mutual coupling between two microstrip patches (Ref. 1) holds experimentally and is discussed in Section 4.5.

A 4 element patch array was designed and is described in Section 5.1. Some near-field measurements were performed; however, results showed that by using a small dipole probe, the amplitude across the aperture of the array could be measured; however, the phase could not be accurately obtained. Thus, a far-field extrapolation would not be made.

A basic design for a Microwave Landing System (MLS) microstrip antenna is described in Section 6. The elevation pattern can be shaped to requirements using a linear array of 32 rectangular patches. Fifty-four of these vertical arrays aligned side-by-side will produce the required azimuth pattern, each of the linear arrays being fed from a corporate feed. The array aperture will have dimensions of 80 inches wide (2032mm) by 48 inches high (1219mm). The performance characteristics of each linear array are expected to be:

Radiation efficiency	:	$\cong$ 70%
VSWR	:	$<$ 1.2
Return Loss	:	$<$ -20 dB
Microstrip Losses	:	$\cong$ 1.1 dB
Power Lost in Load	:	$\cong$ 0.3 dB

The cost factors involved in producing one microstrip antenna will be relatively high since a photographic mask must be produced and production problems resolved. However, it is not expected that this cost will be more than 75% that of a slotted waveguide antenna. For a production of a number of antennas, the cost will be significantly smaller.

In conclusion, it has been shown in this study that a microstrip antenna can be produced to meet the requirements of a MLS azimuth subsystem antenna and that it can be a cheaper alternative to a slotted waveguide antenna. Also, it will be easier to manufacture, be repeatable, and contribute to a more frangible system.

8.0 REFERENCES

1. L. Lewin, Radiation from discontinuities in Strip line, IEEE Monograph No. 358E Feb. 1960, page 163-170.

2. Microstrip Antennas, by I.J. Bahl & P. Bhartion, published by Artech House.

3. Linearly polarized Microstrip Antenna, by Andras G. Derneryd, IEEE Transaction on Antennas & Propogation, Nov. 1976, page 846-851.

4. Hammerstad, E.O. & Bekkadal, F. ' A microstrip hand book', ELAB Report, STF 44 A74169, N7034, University of Trondheim - NTH, Norway, 1975.

5. Microstrip Antennas & arrays pt. 2 - New array design technique, Microswaves, optics & Acoustics, Sept. 1977, Vol 1, No. 5, page 175.

6. A New Travelling Wave Antenna in Microstrip by Wolfgang Menzel, 8th European Microwave Conf. Sept. 1978, page 302-306.

7. Tiuri, M.S. Chain Antennas, IEEE ARS, INT. Symp. Digest, 1974, page 274-277.

8. Ref. 2 page 311.

9. Microstrip Antenna "Theory and Design", by J.R. James, P.S. Hall and C. Wood, Peter Peregrinus LTD Londong, page 24.

10. Ref. 2 page 56.

11. Ref. 3 page 75.

12. Printed Circuit Antenna Technology, page 4-1, proceedings of the workshop, Oct. 17-19, 1979. New Mexico State University, New Mexico.

13. Microstrip lines and Slot lines, by K.C. Cupta, Ramesh Carg and I.J. Bahl, page 137. printed by Artech House.

14. Antenna theory, analysis and design, by Balanis, Harper & Row Publishers, page 684.

15. The Synthesis of Shaped Patterns with Series-Fed Microstrip Patch Arrays, by Bevan B. Jones, Francis Y. M. Chow, and Anthony W. Seets, IEEE Transactions on Antennas and Propagation, Vol. AP-30, No. 6, November 1982, page 1206.

16. Directive Microstrip Antennas, by D. Markopoulos and P. Catechi, 7th European Microwave Conference, 1977, pp. 288-291.

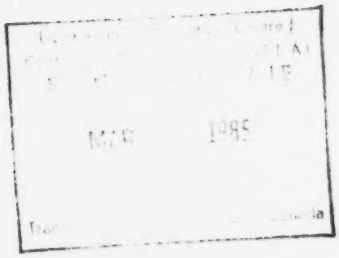

MICROWAVE LANDING SYSTEM (MLS)
MICROSTRIP ANTENNA STUDY
SUMMARY REPORT
TP5437E

Prepared for:
Transportation Development Centre

April 1984

By:

Stuart G. Bailey

Canadian Astronautics Limited

The contents of this report reflect the views of the contractor and not necessarily the official views or policies of the Transportation Development Centre.

Également disponsible en français - TP5437F

REPORT DOCUMENTATION FORM

1 Transport Canada Report No	2 TDC Project No	3 Recipient's Catalogue No
TP5437E	6014	

4 Title and Subtitle	5 Report Date
MICROWAVE LANDING SYSTEM (MLS) MICROSTRIP ANTENNA STUDY - SUMMARY REPORT	April, 1984
	6 Performing Organization Report No

7 Author(s)	8 Transport Canada File No
Stuart G. Bailey	D1455-153-4

9 Performing Organization Name and Address	10 DSS File No
Canadian Astronautics Ltd. 1050 Morrison Dr. Ottawa, Ont. K2H 8K7	12SD.T8200-3-3504
	11 DSS or Transport Canada Contract No OSD83-00041

12 Sponsoring Agency Name and Address	13 Type of Report and Period Covered
Transportation Development Centre (TDC) 1000 Sherbrooke St. West Suite 2421 Montreal, P.Q. H3A 2R3	Summary, July 1983-April 1984
	14 Sponsoring Agency Code

15 Supplementary Notes	16 TDC Project Officer
Summary of "Microwave Landing System (MLS) Microstrip Antenna Study", TP5438E	Micha Avni

17 Abstract

The Microwave Landing System (MLS) defined by the International Civil Aviation Organization is to be the standard instrument for landing aircraft in reduced visibility. At present, the slotted waveguide type antenna has been used to provide the azimuth coverage of the MLS system. However, a microstrip antenna could provide a more cost-effective solution to the problem.

A study of the possiblities of using a microstrip antenna is reported. Various microstrip antenna designs were analyzed and a suitable design was chosen. This design consisted of a linear array of rectangular patch radiators. The rectangular microstrip patch radiator was analyzed theoretically and experimentally, and some design equations were given. The correlation between theory and experiment was good in most cases and Lewin's theory on mutual coupling corresponded well with the experimental measurements made. Finally, a basic design concept was outlined and some typical performance parameters were given.

The patch array antenna proved easy to design and manufacture, providing the correct polarization, gain and VSWR.

This study concludes that a microstrip antenna can be produced to meet the requirements of an MLS azimuth subsystem antenna and that it can be a cheaper alternative to a slotted waveguide antenna. Also, it will be easier to manufacture, be repeatable, and contribute to a more frangible system.

18 Key Words	19 Distribution Statement
MICROWAVE LANDING SYSTEM, MLS MICROSTRIP ANTENNA	Limited number of copies available from Transportation Development Centre

20 Security Classification (of this report)	21 Security Classification (of this page)	22 No. of Pages	23 Price
UNCLASSIFIED	UNCLASSIFIED	10	NIL

TDC/CDT 79-005

FORMULE DE DOCUMENTATION POUR RAPPORT

1 N° du rapport Transports Canada	2 N° de l'étude — CDT	3 N° de catalogue du destinataire
TP5437E	6014	

4 Titre et sous-titre	5 Date du rapport
MICROWAVE LANDING SYSTEM (MLS) MICROSTRIP ANTENNA STUDY SUMMARY REPORT	Avril 1984
	6 N° du rapport de l'organisme exécutant
7 Auteur(s)	8 N° de dossier Transports Canada
Stuart G. Bailey	D1455-153-4
9 Nom et adresse de l'organisme exécutant Canadian Astronautics Ltd. 1050 Morrison Drive Ottawa, Ontario K2H 8K7	10 N° de dossier — ASC 12SD.T8200-3-3504
	11 N° de contrat — ASC ou Transports Canada OSD83-00041
12 Nom et adresse de l'organisme parrain Centre de développement des transports (CDT) 1000 ouest, rue Sherbrooke Suite 2421 Montréal, Québec H3A 2R3	13 Genre de rapport et période visée Sommaire Juillet 1983 - avril 1984
	14 Code de l'organisme parrain 6014
15 Remarques additionnelles Rapport sommaire de TP5438E "Microwave Landing System (MLS) Microstrip Antenna Study"	16 Agent de projet — CDT Micha Avni

17 Résumé

Le système d'atterrissage hyperfréquence est le système standard adopté par l'Organisation de l'aviation civile internationale pour l'atterrissage des aéronefs dans des conditions de visibilité réduite. Actuellement, la couverture azimutale est obtenue à l'aide d'une antenne du type guide d'ondes à fentes. Toutefois, une antenne à microrubans serait moins coûteuse à utiliser.

Les résultats d'une étude sur la possibilité d'utiliser une antenne à microrubans sont rapportés ici. Divers types d'antennes à microrubans ont été examinés et un type approprié a été choisi. Celui-ci est constitué d'un alignement de radiateurs en plaquettes rectangulaires. La plaquette rectangulaire à microrubans a été étudiée théoriquement et expérimentalement et certaines équations de conception sont données. L'accord entre la théorie et l'expérience est bon dans la plupart des cas et la théorie de Lewin sur le couplage mutuel décrit bien les résultats expérimentaux. Enfin, un modèle d'antenne simple est décrit et certains paramètres de performance typiques sont donnés.

L'antenne à alignement de plaquettes s'est révélée facile à concevoir et à fabriquer et procure la polarisation, le gain et le ROS désirés.

La conclusion de cette étude est qu'on peut fabriquer une antenne à microrubans pouvant servir de sous-système d'antenne azimutale hyperfréquence et qu'elle est moins coûteuse qu'une antenne en guide d'ondes à fentes. De plus, de construction simple, elle peut être fabriquée à plusieurs exemplaires et elle est plus frangible.

18 Mots-clés	19 Diffusion
Système d'atterrissage hyperfréquence (MSL). Etude sur les antennes à microrubans.	Le CDT dispose d'un nombre limité de copies

20 Classification de sécurité (de ce rapport)	21 Classification de sécurité (de cette page)	22 Nombre de pages	23 Prix
non-classifié	non-classifiée	10	Nil

CDT/TDC 79-005

1.0 INTRODUCTION

The Microwave Landing System defined by the International Civil Aviation Organization is to be the standard instrument for landing aircraft in reduced visibility. A significant level of effort has been expended by many countries in evaluating and developing these systems.

At the present time the antennae employed are of the slotted waveguide type. These provide a reliable, yet heavy and high cost solution to the problem. An alternative technique, as yet untried, is to use a microstrip antenna.

A further consideration is the frangibility of the antenna. The slotted waveguide antenna is a non-frangible system; however, the microstrip antenna will be a light, inexpensive alternative which would contribute greatly to a frangible system.

The microstrip antenna is formed from a TEM line transmission medium, usually a dielectric sheet with a ground plane on one side and a distribution circuit on the other side. Because of the dielectric the electromagnetic fields are largely contained between the two conductors. Such a system lends itself to photographic techniques and is therefore an inexpensive method when used in production.

2.0 OBJECTIVES

This study was undertaken to determine the feasibility of using a microstrip array antenna in a microwave landing system (MLS).

In this study we set out to cover the following objectives:

(i) Assess alternative microstrip antenna designs

(ii) Determine which microstrip antenna would most easily meet the requirements

(iii) Analyze the chosen microstrip antenna design

(iv) Evaluate this design experimentally

(v) Design and test short linear array

(vi) Outline a basic design for a MLS microstrip antenna

3.0 DISCUSSION

During the course of this study various microstrip antenna designs were analysed and their characteristics evaluated for suitability for a MLS azimuth antenna.

In assessing alternative microstrip designs, a linear array of rectangular patch radiators was chosen as the best candidate for the MLS antenna.

The design has been chosen for its simple shape and ease of manufacture. It can easily be represented by a transmission line model and therefore the amplitude and phase of radiation at each patch can be readily obtained. The amplitude of the radiation sources is determined by the width of the patch and the phase by their position on the line.

A detailed analysis of the chosen design is given in the report covering the important aspects of the patch characteristics.

Rectangular patch antennas were made and experimental measurements made of their characteristics such as insertion loss, return loss, mutual coupling and cross-polarization. It was shown that Lewin's theoretical calculation for mutual coupling between two microstrip patches (Ref. 1) holds experimentally and is discussed in the report.

A 4-element patch array was designed. Some near-field measurements were performed. Results showed that by using a small dipole probe, the amplitude across the aperture of the array could be measured; however, the phase could not be accurately obtained. Thus, a far-field extrapolation could not be made.

A basic design for a Microwave Landing System (MLS) microstrip antenna is described in Section 6 of the report. The elevation pattern can be shaped to requirements using a linear array of 32 rectangular patches. Fifty-four of these vertical arrays aligned side-by-side will produce the required azimuth pattern, each of the linear arrays being fed from a corporate feed. The array aperture will have dimensions of 80 inches wide (2032 mm) by 48 inches high (1219 mm). The performance characteristics of each linear array are expected to be:

Radiation efficiency	:	$\geq$ 70%
VSWR	:	$\leq$ 1.2
Return Loss	:	$\leq$ -20 dB
Microstrip Losses	:	$\geq$ 1.1 dB
Power Lost in Load	:	$\geq$ 0.3 dB

It has already been shown that it is possible to produce a microstrip array which will meet the requirements of an MLS shaped elevation pattern using a design procedure similar to that outlined in the report (Ref. 2).

4.0 CONCLUSION

It has been shown in this study that a microstrip antenna can be produced to meet the requirements of a MLS azimuth subsystem antenna and that it can be a cheaper alternative to a slotted waveguide antenna. Also, it will be easier to manufacture, be repeatable, and contribute to a more frangible system.

The cost factors involved in producing one microstrip antenna will be relatively high since a photographic mask must be produced and production problems resolved. However, it is not expected that this cost will be more than 75% that of a slotted waveguide antenna. For a production of a number of antennas, the cost will be significantly smaller.

REFERENCES

1. L. Lewin, Radiation from discontinuities in Stripline, IEEE Monograph No. 358E Feb. 1960, page 163-170.

2. Bevan B. Jones, Francis Y.M. Chow, and Anthoney W. Sheets, the Synthesis of Shaped Patterns with Series-Fed Microstrip Patch Arrays, IEEE Transactions on Antennas and Propagation, Vol. AP-30, No. 6, Nov. 1982, page 1206.

TP 5520F

SYSTÈME D'ATTERRISSAGE HYPERFRÉQUENCE
ANTENNE DE BALAYAGE AZIMUTAL

RAPPORT SOMMAIRE

par

Micronav Limited

Sydport Industrial Park
Sydney (Nouvelle-Écosse)

Mai 1984

Les opinions exprimées dans ce rapport sont celles des auteurs et ne correspondent pas nécessairement aux opinions ou à la politique officielle du Centre de développement des transports.

Also available in English under the title: "Microwave Landing System - Azimuth Antenna Subsystem", TP 5520E.

GROUPE DE RECHERCHE

Le groupe de recherche chez Micronav Limited était composé de:

J. Currie

M. McAloney

M. Tough

J. Foote

et autres.

REMERCIEMENTS

Les auteurs désirent remercier pour leur aide le personnel de Canadian Astronautics Limited, de Hughes Aircraft Company et, plus particulièrement, celui de Meyer Associates de Boston (Mass.).

FORMULE DE DOCUMENTATION POUR RAPPORT

1 N° du rapport Transports Canada	2 N° de l'étude — CDT	3 N° de catalogue du destinataire
TP 5520F	4977	

4 Titre et sous-titre	5 Date du rapport
SYSTEME D'ATTERRISSAGE HYPERFREQUENCE ANTENNE DE BALAYAGE AZIMUTAL	Mai 1984
	6 N° du rapport de l'organisme executant
7 Auteur(s)	8 N° de dossier Transports Canada
M. McAloney, M. Senechal, M. Tough, J. Whyte	D1455-153-2
9 Nom et adresse de l'organisme executant Micronav Limited Sydport Industrial Park Case postale 1523 Sydney, Nouvelle Ecosse B1P 6R7	10 N° de dossier — ASC 07SC.T8200-2-2599
	11 N° de contrat — ASC ou Transports Canada OSC83-00093
12 Nom et adresse de l'organisme parrain Centre de développement des transports 1000 ouest, rue Sherbrooke Suite 2421 Montréal, Québec H3A 2R3	13 Genre de rapport et période visée Sommaire Mai/83 - Mai/84
	14 Code de l'organisme parrain
15 Remarques additionnelles Sommaire du rapport final "Microwave Landing System Azimuth Antenna Subsystem" TP5519E.	16 Agent de projet — CDT M. Avni

17 Resume

Ce rapport décrit brièvement la mise au point et la construction d'une antenne de balayage azimutal pour système d'atterrissage hyperfréquence (MLS). Une étude a démontré la faisabilité d'un réseau comportant 54 radiateurs en guides d'ondes à fentes, des déphaseurs 4 bits et un réseau d'alimentation à répartiteur de puissance. Les composants ont été fabriqués, évalués et modifiés selon les besoins. Un prototype d'antenne à balayage azimutal a été construit et testé de façon approfondie sur un terrain d'essai. Des circuits de commande et une source hyperfréquence étaient incorporés à l'antenne. Des essais au sol et en vol ont permis de vérifier que le système est conforme aux normes internationales pour le matériel de réception standard utilisé en avionique.

18 Mots-clés	19 Diffusion
Azimut, réseau à commande de phase, guide d'ondes, déphaseur, répartiteur de puissance.	Le CDT dispose d'un nombre limité d'exemplaires.

20 Classification de sécurité (de ce rapport)	21 Classification de sécurité (de cette page)	22 Nombre de pages	23 Prix
non-classifié	non-classifiée	22	Nil

REPORT DOCUMENTATION FORM

1 Transport Canada Report No
TP 5529E

2 TDC Project No
4977

3 Recipient's Catalogue No

4 Title and Subtitle
MICROWAVE LANDING SYSTEM AZIMUTH ANTENNA SUBSYSTEM

5 Report Date
May 1984

6 Performing Organization Code

7 Author(s)
M. McAloney, M. Senechal, M. Tough, J. Whyte

8 Transport Canada File No
DI455-154-2

9 Performing Organization Name and Address
Micronav Limited
Sydport Industrial Park
P.O. Box 1523
Sydney, Nova Scotia B1P 6R7

10 DSS File No
07SC.18200-2-2599

11 DSS or Transport Canada Contract No
05083-000094

12 Sponsoring Agency Name and Address
Transportation Development Centre
1000 Sherbrooke Street West
Suite 2421
Montreal, Quebec H3A 2R3

13 Type of Report and Period Covered
Summary May/83-May/84

14 Sponsoring Agency Code

15 Supplementary Notes
Summary of "Microwave Landing System Azimuth Antenna Subsystem" TP5519E.

16 TDC Project Officer
M. Avnit

17 Abstract

This summary report briefly describes a project to develop and construct an azimuth antenna for a microwave landing system. A feasibility study demonstrated the use of a fully filled array of 54 slotted waveguide radiators, 4-bit phase shifters and a power divider feed network. Individual components were fabricated, evaluated and redesigned as required. A prototype azimuth antenna was constructed and extensively tested on an antenna range. The antenna was integrated with control electronics and a microwave source. Ground and flight testing of the system confirmed compatibility with standard avionics receiving equipment to international standards.

18 Key Words
Azimuth, phased array, waveguide, phase shifters, power divider.

19 Distribution Statement
Limited number of copies available from sponsoring agency

20 Security Classification (of this report)
unclassified

21 Security Classification (of this page)
unclassified

22 No. of Pages
42

23 Price
nil

TDC 0012 (9/85)

AVANT PROPOS

Ce rapport résume sommairement l'élaboration d'une antenne de balayage azimutal pour système d'atterrissage hyperfréquence (MLS). Cette antenne a été mise au point par Micronav Limited pour le Centre de développement des transports, en vue d'être utilisée avec le bloc électronique de commande Micronav pour MLS.

Les principaux objectifs du programme étaient les suivants:

a. élaborer une version préliminaire de l'antenne;

b. démontrer la faisabilité de l'antenne proposée;

c. mettre au point et construire une antenne de balayage azimutal pour MLS;

d. effectuer des essais approfondis à Ottawa, chez le constructeur (Micronav) et au voisinage d'une piste de l'aéroport de Sidney.

Cette étude vise à établir au Canada des compétences en matière de MLS afin d'exploiter les vastes marchés potentiels, tant au niveau national qu'international.

Le système d'atterrissage hyperfréquence permet de guider un aéronef avec précision au moyen d'un ordinateur au moment de l'approche et de l'atterrissage. Le système de balayage azimutal chargé de la couverture horizontale est constitué de deux sous-systèmes: l'antenne et le bloc de commande électronique.

L'antenne balaie électroniquement la zone de couverture au moyen d'un faisceau étroit et fournit une information de position précise à l'aéronef. L'énergie radiofréquence d'une source unique est répartie entre 54 déphaseurs et éléments rayonnants via un répartiteur de puissance (alimentation collective). Les déphaseurs sont commandés numériquement par le bloc de commande électronique afin d'obtenir la distribution de phases désirée sur le réseau d'éléments rayonnants.

Un guide d'ondes distinct, monté au bas des 54 autres guides d'ondes, fournit les échantillons de signal qui permettent de surveiller le fonctionnement du système.

TABLE DES MATIÈRES

1. INTRODUCTION 1
   1.1 Généralités 1
   1.2 Historique 1

2. SYSTÈME DE BALAYAGE AZIMUTAL 4
   2.1 Spécifications 4
   2.2 Fonctionnement du système 5
   2.3 Source hyperfréquence 6
   2.4 Alimentation collective 8
   2.5 Déphaseur 8
   2.6 Réseau à commande de phase 9

3. ESSAIS ET RÉSULTATS 11

4. CONCLUSIONS 12

BIBLIOGRAPHIE 13

LISTE DES FIGURES ET TABLEAU

Figure 1 Fonctionnement de l'antenne de balayage azimutal pour MLS 3
Figure 2 Schéma synoptique du système 7

Tableau 1 Caractéristiques de l'antenne de balayage azimutal pour MLS 4

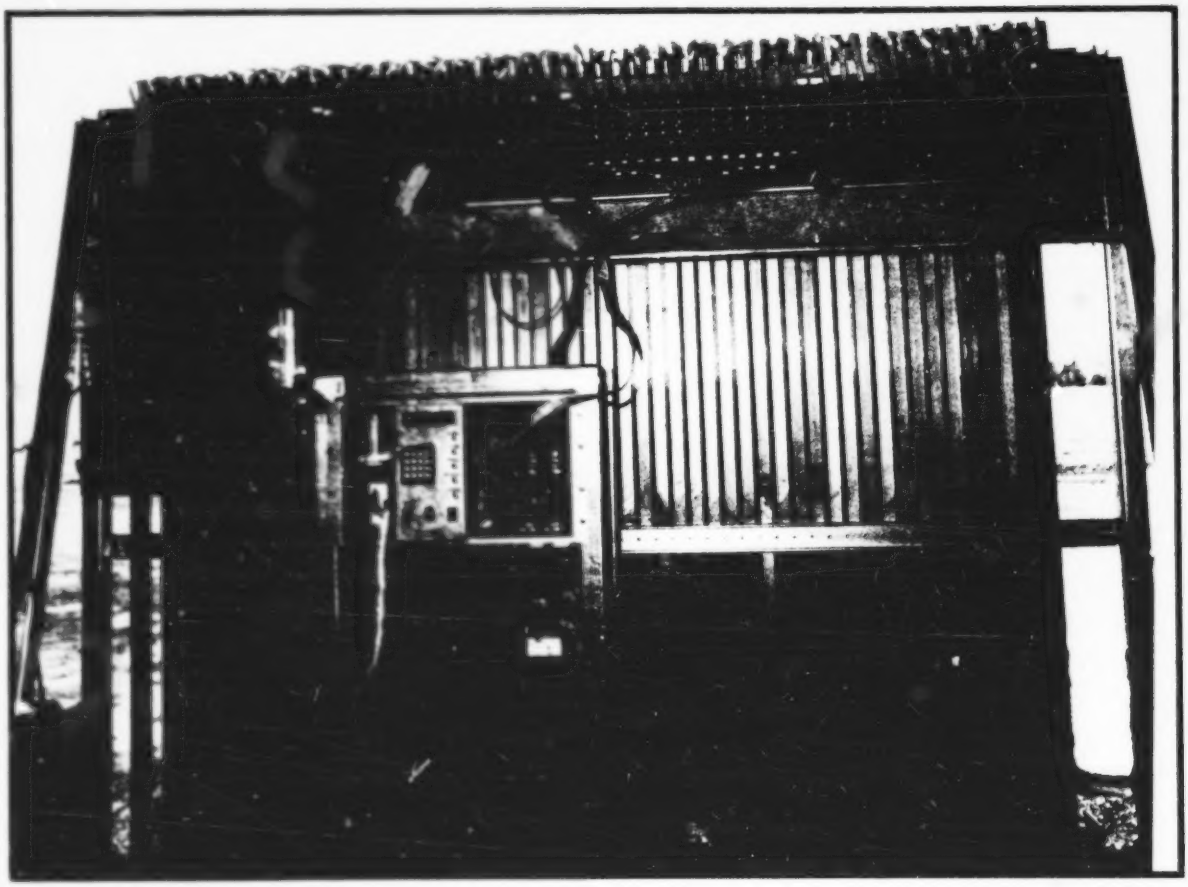

Antenne de balayage azimutal pour MLS avec son bloc de commande électronique (vue arrière)

1. INTRODUCTION

1.1 Généralités

En mai 1983, le Centre de développement des transports a demandé à Micronav Limited de mettre au point et de construire une antenne de balayage azimutal pour système d'atterrissage hyperfréquence. Ce sous-système doit être utilisé conjointement avec le bloc électronique de commande mis au point précédemment.

Avec la réalisation de l'antenne de balayage azimutal, nous avons atteint un jalon important dans l'élaboration de systèmes d'atterrissage hyperfréquence (MLS) de conception entièrement canadienne.

1.2 Historique

Les systèmes d'atterrissage ont pour objet de fournir au personnel d'un aéronef, qui s'apprête à atterrir, des renseignements sur la position de son appareil relativement à la piste et à la trajectoire de descente désirée. On se sert actuellement d'un système d'atterrissage aux instruments (ILS) mis au point durant la Seconde Guerre mondiale. Ce système utilise deux faisceaux radio fixes émis par de grandes antennes placées près de la piste. Un récepteur installé dans l'habitacle de l'aéronef capte ces faisceaux et en déduit l'écart latéral et l'angle de descente. Les systèmes d'atterrissage aux instruments manquent de souplesse: ils ne peuvent fournir qu'un seul trajet d'approche quels que soient le type de l'aéronef ou les autres conditions. Leur installation est coûteuse; de plus, ils ne peuvent pas être utilisés sur tous les types de terrain et n'offrent que 40 canaux distincts.

Le système d'atterrissage hyperfréquence (MLS) a été choisi par l'Organisation de l'aviation civile internationale (OACI) comme système standard universel pour le guidage des aéronefs à l'atterrissage. Le plan de l'OACI prévoit le remplacement des ILS par les MLS durant une période de 10 ans, commençant en 1985.

Le MLS présente plusieurs avantages qui en font le système du futur et rendent l'ILS désuet; ce sont:

a. une performance et une précision améliorées;

b. la possibilité de desservir des endroits comme les régions montagneuses et les plates-formes de forage flottantes;

c. une sécurité accrue;

d. une multiplicité de trajets d'approche pour les hélicoptères, les aéronefs ordinaires et les ADAC à voilure fixe;

e. un nombre accru de canaux disponibles (200);

f. des économies de carburant résultant de trajets d'approche plus courts et des piles d'attente réduites;

g. un aménagement minimal du site;

h. la possibilité d'atterrissage automatique;

i. une installation peu coûteuse;

j. une insensibilité beaucoup plus grande à la nature du terrain.

Le contractant choisi pour ce projet, Micronav Limited, a été incorporé en décembre 1980 dans le but de mettre au point un système d'atterrissage hyperfréquence. À l'heure actuelle, un système de balayage azimutal a été réalisé et une antenne de balayage vertical est en voie d'élaboration. Des sous-contrats ont été accordés à la Hughes Aircraft Company pour une étude de faisabilité sur un prototype et à la Canadian Astronautics Limited pour la conception et la fabrication de l'antenne.

L'antenne de balayage azimutal a pour fonction d'émettre un faisceau de 2° de largeur qui balaie l'horizon dans les deux sens à une vitesse angulaire constante de 20 000°/seconde entre des limites de couverture de ±40° de part et d'autre de la ligne médiane de la piste. Un récepteur MLS installé dans l'aéronef mesure la durée entre le passage du faisceau dans un sens et son passage lorsqu'il revient dans l'autre sens. Le balayage de gauche à droite lorsqu'on se place derrière l'antenne est le balayage horaire. Dans l'autre sens, de droite à gauche, le balayage est dit antihoraire. Le chronométrage commence au moment où le faisceau de balayage horaire passe par le récepteur dans le sens horaire et se termine lorsque le faisceau passe par le récepteur dans le sens antihoraire. La durée du chronométrage sera plus longue pour un aéronef à droite de la ligne médiane de la piste que pour un aéronef à gauche de

cette ligne. La figure 1 illustre le fonctionnement de l'antenne de balayage azimutal.

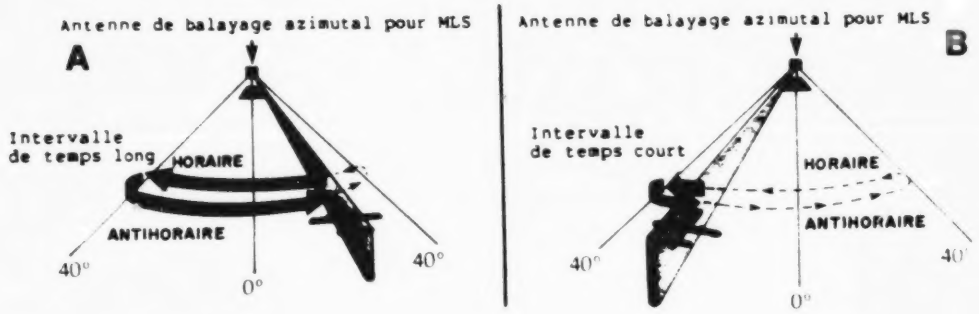

Figure 1 Fonctionnement de l'antenne de balayage azimutal pour MLS

Le temps mesuré est décodé par le récepteur MLS pour déterminer l'angle d'approche de l'aéronef par rapport à la piste. Ce trajet est comparé avec le trajet désiré, choisi par le pilote, afin de lui indiquer s'il doit diriger l'aéronef vers la droite ou vers la gauche. Le pilote peut choisir un angle d'approche quelconque dans la zone de couverture, ce qui lui permet de faire une approche curviligne ou une approche en ligne droite. Les MLS ayant recours à cette différence entre intervalles de temps sont des systèmes à faisceau battant à référence temporelle.

2. SYSTÈME DE BALAYAGE AZIMUTAL

2.1 Spécifications

L'antenne de balayage azimutal MLS émet un faisceau étroit en éventail qui balaie le plan azimutal dans les deux sens.

Les caractéristiques générales de l'antenne de balayage azimutal sont comme suit:

Tableau 1 Caractéristiques de l'antenne de balayage azimutal pour MLS

Gamme de fréquences (bande passante)	5030-5090 MHz
Angle de balayage maximal	±42° (azimut)
Largeur du faisceau à 5060 MHz	2,0° dans le plan de balayage
Niveau de crête des lobes latéraux	-20 dB dans le plan de balayage
Gain du réseau	28 dB
Puissance maximale admissible	10 watts
Vitesse angulaire du faisceau	20 000°/seconde
Gamme de températures de fonctionnement	±65°C

Le système de balayage azimutal doit aussi satisfaire aux conditions suivantes:

1. fonctionnement sans dégradation de performance dans des conditions atmosphériques rigoureuses;
2. grande fiabilité;
3. prix modique;
4. facilité d'entretien par un personnel approprié.

2.2 Fonctionnement du système

Micronav en est venu à la conclusion qu'un réseau à commande de phase était le meilleur type d'antenne pour un MLS. Le fonctionnement de chacune des parties du système est décrit ci-dessous.

a. Source hyperfréquence

L'énergie hyperfréquence est fournie à l'antenne par la source hyperfréquence. Celle-ci est constituée d'un amplificateur de puissance, d'un excitateur, d'un modulateur de phase différentielle et d'un commutateur bipolaire bidirectionnel pouvant fournir une puissance RF de 10 watts sur le canal choisi dans la gamme de fréquences MLS.

b. Alimentation collective

L'alimentation collective divise le signal de sortie de la source hyperfréquence en 54 signaux, un pour chacun des éléments rayonnants du réseau d'antenne. Pour obtenir le diagramme de rayonnement désiré, le signal est divisé de façon à obtenir des signaux de sortie de même phase dans une distribution d'amplitude spécifique.

c. Déphaseurs

Les déphaseurs permettent de contrôler individuellement la phase de chacun des signaux de sortie de l'alimentation collective. Montés entre l'alimentation collective et les éléments rayonnants, ils permettent de diriger le faisceau à l'angle de balayage azimutal désiré.

d. Éléments rayonnants

Les éléments rayonnants, au nombre de 54, sont constitués d'antennes à fentes montées verticalement. Chaque élément a un diagramme de rayonnement dans le plan vertical et un large diagramme dans le plan azimutal. Ces diagrammes de rayonnement produisent un faisceau étroit d'une largeur de 2 degrés lorsqu'ils sont combinés ensemble.

e. Contrôleur

Le contrôleur, qui est un guide d'ondes installé horizontalement, reçoit un signal de chacun des 54 éléments rayonnants. Ces signaux sont ajoutés les

uns aux autres pour donner un signal composite qui est ensuite soumis à une analyse.

f. Antenne d'identification

L'antenne d'identification transmet les données à modulation de phase différentielle lesquelles fournissent l'information sur le site requise par le récepteur MLS à bord de l'aéronef.

g. Bloc de commande électronique

Le bloc de commande électronique est constitué par les circuits qui engendrent tous les signaux d'horloge et de données et qui commandent les déphaseurs durant le balayage.

On trouvera à la figure 2 un schéma synoptique des diverses parties du système.

2.3 Source hyperfréquence

La source hyperfréquence excite les éléments rayonnants en fournissant aux déphaseurs une onde entretenue de 10 watts, par le truchement du répartiteur de puissance (alimentation collective). Les principaux éléments de la source sont un amplificateur de puissance à transistors à effet de champ à GaS Fujitsu Microelectronics et un excitateur Frequency West. Celui-ci donne une fréquence spécifique déterminée par un cristal interne. L'instabilité ne doit pas dépasser ±10 kHz. Un essai sur une période de deux heures a démontré que l'instabilité était de 150 Hz à température ambiante. La sortie de l'excitateur est protégée par un isolateur. Celui-ci empêche les défaillances, les courts-circuits ou les circuits ouverts d'endommager l'excitateur.

On utilise un déphaseur pour la modulation en phase différentielle des données transmises par l'antenne d'identification. Le déphaseur n'est utilisé que durant la période où cette antenne est en mode d'émission; lorsqu'elle ne rayonne pas, un commutateur est actionné pour empêcher toute fuite d'énergie hyperfréquence vers l'amplificateur. Ce dernier est muni d'un isolateur interne et, par conséquent, ne nécessite pas d'isolateur externe comme c'est le cas pour l'excitateur. L'amplificateur alimente un commutateur bipolaire bidirectionnel dont toutes les sorties peuvent servir de sources. Présentement, deux sorties seulement sont utilisées, l'une pour le réseau de balayage azimutal à commande de phase et l'autre pour l'antenne d'identification. Les deux autres sorties, actuellement

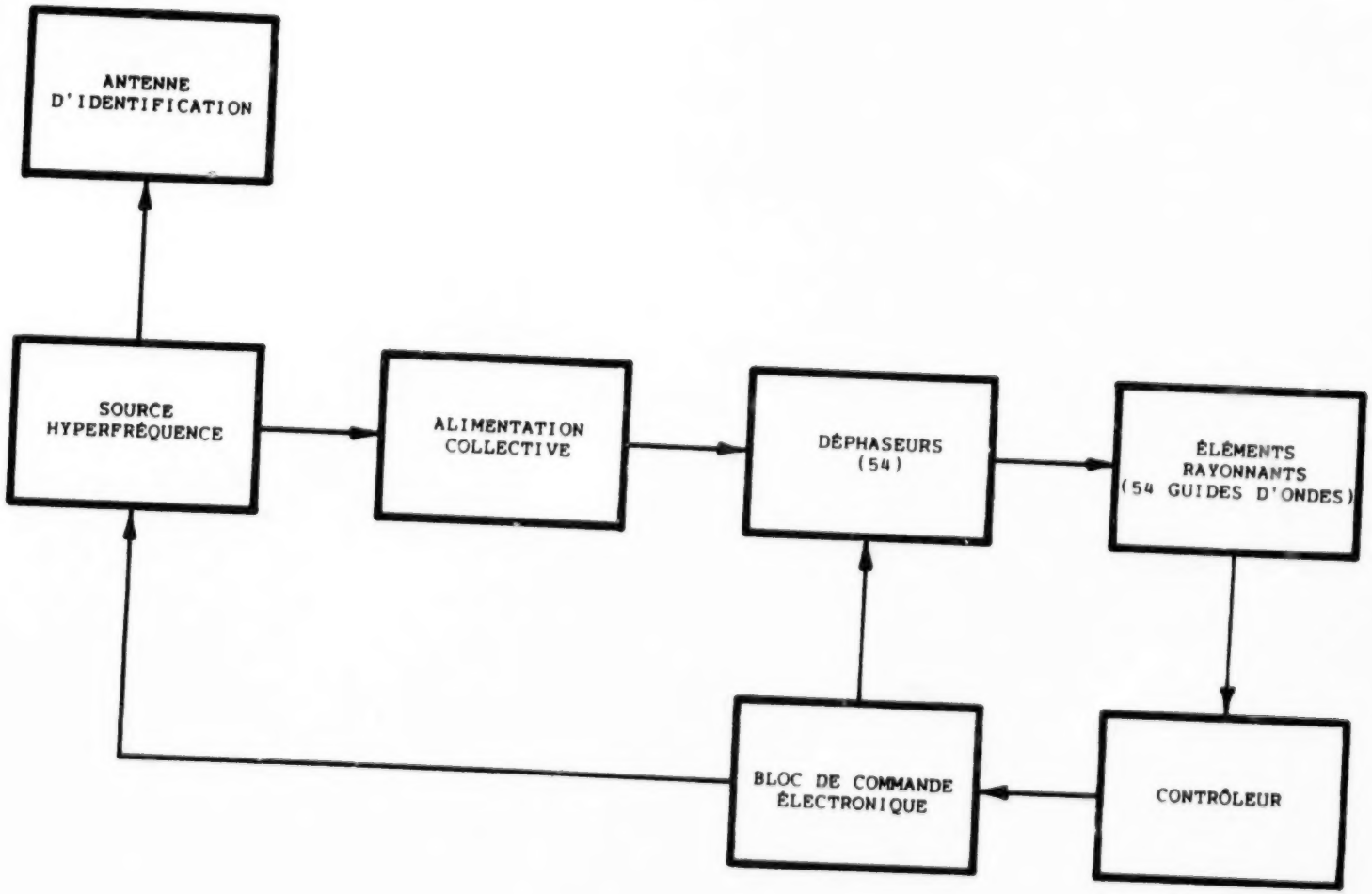

Figure 2 Schéma synoptique du système

munies de charges fictives, peuvent être utilisées pour des antennes indicatrices fonctionnant hors couverture.

Les signaux destinés aux commutateurs d'alimentation hyperfréquence et les signaux de données destinés aux modulateurs à phase différentielle sont fournis par le bloc de commande électronique.

2.4 Alimentation collective

L'alimentation collective doit diviser l'énergie fournie par la source hyperfréquence entre les 54 radiateurs avec une distribution d'amplitude de 30 dB suivant une loi de Taylor N=4.

On a choisi une configuration en parallèle pour l'alimentation collective en raison de la symétrie de cette configuration et de la longueur uniforme des trajets RF entre l'entrée et les sorties. Des diviseurs en "T fendu" modifiés ont été utilisés comme répartiteurs de puissance. Un diviseur en "T fendu" est un dispositif compact et simple fournissant deux signaux de sortie isolés de même phase, mais d'amplitudes inégales, avec une bonne adaptation à chaque porte. Le rapport d'ondes stationnaires d'entrée du diviseur en "T fendu" a été amélioré au moyen d'un transformateur à deux seuils monté à l'entrée. Les rapports de répartition de puissance nécessaires pour donner la distribution de Taylor ont été obtenus en modifiant l'impédance de différentes lignes de transmission dans les répartiteurs de puissance en "T fendu" individuels.

Des microrubans ont été utilisés pour les circuits afin d'éviter le coût élevé et la complexité des alimentations coaxiales ou à guide d'ondes. Les dimensions imposées aux circuits d'alimentation collective exigeaient que les circuits soient déposés sur deux feuilles du substrat en téflon imprégné de verre.

Il a fallu un ajustage d'appoint élaboré des microrubans pour obtenir la performance désirée de l'alimentation collective. Les améliorations futures du système d'alimentation porteront sur la réduction du poids et l'amélioration de la performance.

2.5 Déphaseur

Le déphaseur doit retarder le signal de sortie par rapport au signal d'entrée en le déphasant de 0 à 360° par quantités discrètes. Micronav a établi que, pour un rendement optimal, il fallait utiliser des déphaseurs 4 bits avec un déphasage minimal de 22,5°.

Le déphasage peut être obtenu au moyen de diodes PIN ou de dispositifs ferrite. Les diodes PIN ont été choisies en raison de leur réciprocité, de leur grande vitesse de commutation et de leur compatibilité avec les circuits à microruban. C'est un circuit hybride du type à réflection qui a été choisi pour établir chaque bit de déphasage car ce type de circuit requiert seulement deux diodes et une ligne de contrôle par bit et, de plus, peut être utilisé avec un déphasage quelconque.

Les déphaseurs sont construits sur un substrat en Duroid par pulvérisation cathodique de cuivre dans des configurations aux lignes très exactement définies. Des onglets incorporés aux déphaseurs ont été taillés pour régler la phase de chaque bit et la phase absolue du dispositif. L'utilisation de déphaseurs réglés de façon à avoir la même phase absolue permet d'interchanger ceux-ci et de simplifier la maintenance du système.

Les tests ont démontré que le déphasage avait une erreur de phase "RMS" de 2 degrés, ce qui est inférieur à la tolérance de 4 degrés de la spécification originale. Cette amélioration est le résultat du soin apporté à la conception du déphaseur pour ce qui a trait aux tolérances. L'affaiblissement d'insertion en delta est légèrement plus élevée que la valeur requise, mais cet effet est contrebalancé par la réduction de l'erreur de phase.

Pour réduire le prix de revient et accroître la performance du déphaseur, on pourrait chercher des améliorations dans les directions suivantes:

1. une méthode de fabrication simplifiée utilisant un substrat avec conducteur;

2. le traçage du circuit sur le substrat par gravure à mouillage, technique peu coûteuse;

3. l'utilisation de configurations mieux définies pour réduire les opérations de taillage des onglets lors de l'ajustage d'appoint de la phase;

4. une conception améliorée permettant de réduire le prix de revient.

2.6 Réseau à commande de phase

Les éléments du réseau à commande de phase émettent le faisceau étroit désiré. On a choisi des radiateurs en guide d'ondes à fentes en raison de leur encombrement réduit, de leur robustesse, de leur faible atténuation d'insertion et

de leur grande insensibilité aux variations de température. La position, l'angle et le nombre des fentes déterminent le diagramme de rayonnement d'un guide d'ondes à fentes, la phase, l'amplitude et la fréquence du signal d'entrée étant données. Les éléments rayonnants ont été conçus selon la méthode des fentes résonantes à espacement non uniforme. La phase dépend alors de l'espacement entre les fentes et l'amplitude dépend de l'angle des fentes.

On a obtenu le diagramme de rayonnement azimutal désiré en utilisant la distribution de Taylor qui donne un diagramme théorique offrant le meilleur compromis entre la largeur du faisceau et le niveau des lobes latéraux. Pour un niveau de 30 dB, il faut 54 éléments rayonnants espacés de 3 609 cm. On a eu recours à la méthode de synthèse des diagrammes de rayonnement de Woodward pour donner la forme désirée au faisceau dans le plan vertical.

Les fentes ont été taillées dans un tube d'aluminium WR187 au moyen d'une fraiseuse à commande numérique. Le guide d'ondes reçoit l'énergie hyperfréquence des déphaseurs via des câbles semi-rigides identiques et une section d'attaque. Chaque guide d'ondes est muni d'une charge terminale spéciale construite dans sa base. Des vis de réglage ont été incorporées aux guides d'ondes pour l'adaptation et le réglage de la phase absolue afin d'obtenir des éléments rayonnants interchangeables.

Un contrôleur est incorporé au système; il analyse un échantillon du signal émis pour déterminer s'il y a une défaillance du système. Le contrôleur est constitué d'un segment de guide d'ondes placé horizontalement à la base du réseau à commande de phase. Dans chaque guide d'ondes, la paroi est taillée au bas afin que le contrôleur puisse s'adapter à égalité avec les surfaces intérieures du guide d'ondes. Ceci permet à l'énergie hyperfréquence de pénétrer dans les fentes taillées dans le contrôleur. Celles-ci sont conçues de façon que le contrôleur reçoive la même quantité d'énergie de chacun des éléments du réseau.

3. ESSAIS ET RÉSULTATS

Les essais ont eu lieu au terrain d'essais du laboratoire David Florida du Centre de recherche sur les communications, près d'Ottawa. On a tracé les diagrammes de rayonnement de l'antenne pour vérifier la performance de cette dernière. Il y a eu aussi d'autres tests à Micronav et à l'aéroport de Sidney.

Les essais en vol par le ministère des Transports ont été commencés sans toutefois être complétés en raison de défaillances dans le matériel de l'aéronef; certaines vérifications en vol ont été effectuées et le ministère des Transports a répété les essais au sol effectués par Micronav. Les essais en vol devraient être terminés ce mois-ci; une copie des données sera envoyée à Micronav.

Des essais approfondis au sol ont démontré que l'antenne de balayage azimutal Micronav pour MLS satisfait ou dépasse les exigences de l'Annexe 10 et des normes et pratiques recommandées par l'OACI pour les signaux électromagnétiques.

L'antenne a fonctionné raisonnablement bien en toutes circonstances. L'écart le plus important par rapport à la performance prévue s'est produit dans le niveau (plus élevé que prévu) des lobes latéraux. Les mesures ont indiqué que la largeur du faisceau et la forme des diagrammes de rayonnement étaient conformes aux exigences. La précision du pointage azimutal était aux limites de précision des appareils de mesure.

Les éléments individuels du système de balayage pourraient être améliorés de diverses façons pour donner de meilleurs résultats. En général, ceci se traduirait par des tolérances de production moins rigoureuses et réduirait les opérations de réglage d'appoint et d'ajustage, d'où un prix de revient moins élevé pour le produit final.

4. CONCLUSIONS

Une antenne de balayage azimutal pour MLS a été conçue puis construite et des essais ont démontré qu'elle était conforme aux normes de l'Annexe 10 de l'OACI. Le système de balayage est opérationnel et des essais au sol et en vol ont prouvé qu'il se compare de façon excellente aux systèmes actuels. Une analyse détaillée de la performance globale de l'antenne justifie la modification de certains paramètres initiaux en vue d'obtenir un résultat final satisfaisant.

D'autres travaux sont nécessaires pour adapter les divers composants en vue de leur fabrication. Il serait souhaitable de réduire le poids et les dimensions du système ainsi que le niveau des lobes latéraux, mais ces améliorations n'auraient qu'un effet minimal sur la performance pour ce qui est de l'utilisateur.

BIBLIOGRAPHIE

Balonis, C.A. "Antenna Theory, Analysis and Design", Harper and Row, 1982.

Canadian Astronautics Limited "Report on a Microwave Landing System Antenna", Novembre 1983.

Canadian Astronautics Limited, "Report on Phase II Microwave Landing System Antenna", Mars 1983.

Canadian Astronautics Limited "The Final Report for an Azimuth Microwave Landing System", Février 1984.

Edwards, T.C. "Foundations for Microstrip Circuit Design", John Wiley and Sons, 1981.

Federal Aviation Administration "Microwave Landing System Ground Equipment", FAA-E-2721/ 1a, 2a, 3b, 4a, 5a, Octobre 1983.

Federal Aviation Administration "Microwave Landing System (MLS) Interoperability and Performance Requirements", FAA-STD-022b, Octobre 1983.

Hughes Aircraft Company "Antenna Conceptual Design Study", Mai 1981.

Organisation civile internationale: "Télécommunications aéronautiques", Juillet 1972.

Porad, L.I. and Moynihan, R.L.: "Split-Tee Power Divider", IEEE Transactions on Microwave Theory and Techniques, Septembre 1964.

White, J.F. "Diode Phase Shifters for Array Antennas", IEEE Transactions on Microwave Theory and Techniques, Février 1974.